Phenomenological Analysis of $B \rightarrow PP$ Decays with QCD Factorization *

Dongsheng Du 1,2 Haijun Gong 2 Junfeng Sun 2 Deshan Yang 2 Guohuai Zhu 2

1. CCAST (World Laboratory), P.O.Box 8730, Beijing 100080, China

2. Institute of High Energy Physics, Chinese Academy of Sciences, P.O.Box 918(4), Beijing 100039, China †‡

August 17, 2001

Abstract

In this paper, we study the nonleptonic charmless B decays to two light pseudoscalar mesons within the frame of QCD factorization, including the contributions from the chirally enhanced power corrections and weak annihilation. The predictions for the CP-averaged branching ratios and CP-violating asymmetries are given. Within the reasonable range of the parameters, we find that our predictions for the branching ratios of $B \to PP$ are consistent with the present experimental data. But due to the logarithmic divergences at the endpoints in the hard spectator scatterings and weak annihilation, there are still large uncertainties in these predictions.

PACS numbers 13.25.Hw 12.38.Bx

^{*}Supported in part by National Natural Science Foundation of China and State Commission of Science and Technology of China

[†]Mailing address

 $^{^{\}ddagger}$ Email:duds@mail.ihep.ac.cn, gonghj@mail.ihep.ac.cn, sunjf@mail.ihep.ac.cn, yangds@mail.ihep.ac.cn, zhugh@mail.ihep.ac.cn

1 Introduction

In the standard model (SM), CP violation and quark mixing are closely related to each other. The unitarity of the Cabibbo-Kobayashi-Maskawa (CKM) matrix implies various relations among its elements. The most commonly studied is: $V_{ud}V_{ub}^* + V_{cd}V_{cb}^* + V_{td}V_{tb}^* = 0$, which can be described by a "unitarity triangle" in the complex plane. The study of B meson decays is mainly to make enough independent measurements of the sides and angles of this unitarity triangle. For example, in principle, we can extract or give a constraint for the angle α from the decay $B \to \pi\pi$, and the angle γ from $B \to \pi\pi$ and πK . Therefore, a clear understanding of exclusive non-leptonic charmless B decays can give some useful informations about CKM matrix elements.

Experimentally, many B experiment projects have been running (CLEO, BaBar, Belle etc.), or will run in forthcoming years (BTeV, CERN LHCb, DESY HeraB etc.). Several experimental groups have reported their latest results recently [1, 2, 3], and more B decay channels will be measured with great precision soon. Among these decay channels, quite a few are nonleptonic charmless two-body modes, such as $B \to \pi K$, $\pi \pi$, $K \eta'$ etc.. With the accumulation of the experimental data, the theoretis are urged to gain a deep sight into rare hadronic B meson decays, and to reduce the theoretical errors in determining the CKM parameters from the experimental data.

Theoretically, nonleptonic charmless two-body B decays have been widely discussed and carefully studied in the framework of the effective Hamiltonian and factorization hypothesis. The effective Hamiltonian is obtained by the operator product expansion (OPE) and the renormalization group (RG) method, and generally expressed by the products of the Wilson coefficients and the effective operators which are in forms of the four-quarks operators and magnetic moment operators. The Wilson coefficients can be calculated reliably by the perturbation theory. And, in the SM, they have been evaluated to the next-to-leading order[4]. Thus, the main task for us is to compute the hadronic matrix elements of the effective operators. However, due to the complexity of QCD dynamics, it does not allow us to compute them directly from first principles. Generally, we must resort to the factorization approximation[5] by neglecting the soft interactions between the ejected meson and recoiled system. Under the factorization approximation, the hadronic matrix element of the effective operator can be parameterized into the product of the meson decay constant and meson-meson transition form factor. The comprehensive analysis for nonleptonic charmless two-body B decays based on the naive factorization and/or generalized factorization were done in past decade, and achieved great success.

The factorization approximation does hold in the limit that the soft interactions in the initial and final states can be ignored. It seems that the argument of color-transparency can give reasonable support to the above $\liminf[6]$. Because b quark is heavy, the quarks from b quark decay move so fast that a pair of quarks in a small color-singlet object decouple from the soft interactions. But for the case of the naive factorization, the shortcomings are obvious. First, the renormalization scheme and scale dependence in the hadronic matrix elements of the effective operators are apparently missed. Then the full decay amplitude predicted by the BSW model remains dependent on the renormalization scheme and scale, which are mainly from the Wilson coefficients. In past years, many researchers generalized the naive factorization scheme and made many remarkable progresses, such as the scheme and scale independent effective Wilson coefficients[7], effective color number which is introduced to compensate the 'non-factorizable' contributions, etc.. Furthermore,

some progresses in nonperturbative methods, such as lattice QCD, QCD sum rule etc. [8, 9, 10], allow us to compute many non-perturbative parameters in B decays, such as the meson decay constants and meson-meson transition form factors. Every improvement allows us to have a closer look at the B nonleptonic decays. In the literature [11, 12], the authors gave the comprehensive and detailed analysis for the nonleptonic two-body charmless B decays within the frame of the generalized factorization.

Two year ago, Beneke, Buchalla, Neubert, and Sachrajda (BBNS) gave a QCD factorization formula in the heavy quark limit for the decays $B \to \pi\pi[13]$. They pointed out that the radiative corrections from hard gluon exchange can be calculated by use of the perturbative QCD method if one neglects the power contributions of Λ_{QCD}/m_b . This factorization formula can be justified in the case that the ejected meson from the bquark decay is a light meson or an onium, no matter whether the other recoiling meson which absorbs the spectator quark in B meson is light or heavy. But for the case that the ejected meson is in an extremely asymmetric configuration, such as D meson, this factorization formula does not hold. The contributions from the hard scattering with the spectator quark in B meson are also involved in their formula. This kind of contribution cannot be contained in the naive factorization. But it appears in the order of α_s . So they said that the naive factorization can be recovered if one neglects the radiative corrections and power Λ_{QCD}/m_b suppressed contributions in the QCD factorization, and the 'nonfactorizable' contributions in the naive factorization can be calculated perturbatively, so we do not need a phenomenological parameter N_c^{eff} to compensate the 'non-factorizable' effects. Moreover, because b quark mass is not very large in the reality, the potential power corrections, in particular, the chirally enhanced corrections will play an important role in $B \to PP[14, 15, 16]$. So the twist-3 light-cone wave function of the light pseudoscalar must be taken into account. Unfortunately, QCD factorization breaks down at twist-3 level. There is a logarithmic divergence in the hard spectator scattering at the endpoint of the twist-3 light-cone distribution amplitude (LCDA). However, we still can parameterize this divergence by some reasonable parameters.

Phenomenologically, this QCD factorization (BBNS approach) has been applied to study many B meson decay modes, such as $B \to D^{(*)}\pi^-[17, 18], \pi\pi, \pi K[19, 20, 14, 16]$ and other interesting channels [21, 22, 23, 25]. Especially, recent paper [16] by Beneke et al. about $B \to \pi\pi$ and πK gives a complete conceptual and technical description for the latest development of QCD factorization, and a detailed phenomenological analysis for $B \to \pi\pi$ and πK , in which the contributions from weak annihilation are also taken into account. In this work, we will apply QCD factorization to all modes that B decays into two light pseudo-scalar mesons, and give a careful and detailed analysis. For the decay modes $B \to \pi\pi$ and πK , our work is equivalent to a re-check of Beneke et al.[16], and we find that our results is consistent with theirs. For $B \to P\eta^{(\prime)}$, it has been also done by M. Z. Yang and Y. D. Yang within the frame of QCD factorization[21]. The differences between their work and ours are: we take the other type twist-3 light-cone distribution amplitude ϕ_{σ} into account which makes our results gauge independent, and the the weak annihilation is also considered in our work. On the other hand, the di-gluon mechanism for the production of $\eta^{(\prime)}$ is taken into account in their work. Generally, it is believed that the anomalous coupling of $\eta' g^* g^*$ can account for the large branching ratio of $B \to K\eta'$. However, whether the form factor $\eta^{(\prime)}g^*g^*$ is pertubative or not is still a open question, particularly the virtualities of the two gluons are both soft at the endpoint of the light-cone distribution amplitudes, whether the soft contributions can be suppressed

by the light-cone distribution amplitudes is questionable. Therefore, in our work, di-gluon mechanism is not considered though it can enhance the branching ratio of $B \to K\eta'$. For $B \to KK$, our work is totally new, the study of these decay modes can give a constraint to the endpoint divergence in the weak annihilation.

This paper is organized as follows: in Sect. II, we give a brief review of the effective Hamiltonian and QCD factorization including the chirally enhanced power corrections and weak annihilation; for a quantitative analysis of $B \to PP$, the necessary input parameters are discussed in Sect. III; in Sect. IV, the numerical results of the CP-averaged branching ratios and CP asymmetries for $B \to PP$ are given; Sect. V is devoted to the conclusions.

2 Theoretical frame for B rare decays

2.1 The Effective Hamiltonian

B decays involve three characteristic scales which are strongly ordered: $m_W \gg m_b \gg \Lambda_{QCD}$. How to separate or factorize these three scales is the most essential question in B hadronic decays.

With the operator product expansion method (OPE), the relevant $|\Delta B| = 1$ effective Hamiltonian is given by [4]:

$$\mathcal{H}_{eff} = \frac{G_F}{\sqrt{2}} \left[\sum_{q=u,c} v_q \left(C_1(\mu) Q_1^q(\mu) + C_2(\mu) Q_2^q(\mu) + \sum_{k=3}^{10} C_k(\mu) Q_k(\mu) \right) - v_t \left(C_{7\gamma}(\mu) Q_{7\gamma}(\mu) + C_{8G}(\mu) Q_{8G}(\mu) \right) \right] + h.c., \tag{1}$$

where $v_q = V_{qb}V_{qd}^*$ (for $b \to d$ transition) or $v_q = V_{qb}V_{qs}^*$ (for $b \to s$ transition) and $C_i(\mu)$ are the Wilson coefficients which have been evaluated to next-to-leading order approximation with the perturbation theory and renormalization group method.

In the Eq.(1), the four-quark operators Q_i are given by

$$Q_{1}^{u} = (\bar{u}_{\alpha}b_{\alpha})_{V-A}(\bar{q}_{\beta}u_{\beta})_{V-A} \qquad Q_{1}^{c} = (\bar{c}_{\alpha}b_{\alpha})_{V-A}(\bar{q}_{\beta}c_{\beta})_{V-A}
Q_{2}^{u} = (\bar{u}_{\alpha}b_{\beta})_{V-A}(\bar{q}_{\beta}u_{\alpha})_{V-A} \qquad Q_{2}^{c} = (\bar{c}_{\alpha}b_{\beta})_{V-A}(\bar{q}_{\beta}c_{\alpha})_{V-A}
Q_{3} = (\bar{q}_{\alpha}b_{\alpha})_{V-A} \sum_{q'}(\bar{q}'_{\beta}q'_{\beta})_{V-A} \qquad Q_{4} = (\bar{q}_{\beta}b_{\alpha})_{V-A} \sum_{q'}(\bar{q}'_{\alpha}q'_{\beta})_{V-A}
Q_{5} = (\bar{q}_{\alpha}b_{\alpha})_{V-A} \sum_{q'}(\bar{q}'_{\beta}q'_{\beta})_{V+A} \qquad Q_{6} = (\bar{q}_{\beta}b_{\alpha})_{V-A} \sum_{q'}(\bar{q}'_{\alpha}q'_{\beta})_{V+A} \qquad , \qquad (2)
Q_{7} = \frac{3}{2}(\bar{q}_{\alpha}b_{\alpha})_{V-A} \sum_{q'}e_{q'}(\bar{q}'_{\beta}q'_{\beta})_{V+A} \qquad Q_{8} = \frac{3}{2}(\bar{q}_{\beta}b_{\alpha})_{V-A} \sum_{q'}e_{q'}(\bar{q}'_{\alpha}q'_{\beta})_{V+A}
Q_{9} = \frac{3}{2}(\bar{q}_{\alpha}b_{\alpha})_{V-A} \sum_{q'}e_{q'}(\bar{q}'_{\beta}q'_{\beta})_{V-A} \qquad Q_{10} = \frac{3}{2}(\bar{q}_{\beta}b_{\alpha})_{V-A} \sum_{q'}e_{q'}(\bar{q}'_{\alpha}q'_{\beta})_{V-A}$$

and

$$Q_{7\gamma} = \frac{e}{8\pi^2} m_b \bar{q}_{\alpha} \sigma^{\mu\nu} (1 + \gamma_5) b_{\alpha} F_{\mu\nu}, \quad Q_{8G} = \frac{g}{8\pi^2} m_b \bar{q}_{\alpha} \sigma^{\mu\nu} t^a_{\alpha\beta} (1 + \gamma_5) b_{\beta} G^a_{\mu\nu}, \quad (q = d \text{ or } s). \quad (3)$$

Here Q_1^q and Q_2^q being the tree operators, $Q_3 - Q_6$ the QCD penguin operators, $Q_7 - Q_{10}$ the electroweak penguin operators, and $Q_{7\gamma}$, Q_{8G} the magnetic-penguin operators.

In this effective Hamiltonian for B decays, the contributions from large virtual momenta of the loop corrections from scale $\mu = \mathcal{O}(m_b)$ to m_W are attributed to the Wilson coefficients, and the low energy contributions are fully incorporated into the matrix elements

Table 1: Wilson coefficients in NDR scheme. The input parameters in numerical calculations are fixed: $\alpha_s(m_Z) = 0.1185$, $\alpha_{em}(m_W) = 1/128$, $m_W = 80.42 \text{GeV}$, $m_Z = 91.188 \text{GeV}$, $m_t = 168.2 \text{GeV}$, $m_b = 4.6 \text{GeV}$.

	$\mu = m_b/2$	$\mu = m_b$	$\mu = 2m_b$
C_1	1.136	1.080	1.044
C_2	-0.283	-0.181	-0.105
C_3	0.021	0.014	0.009
C_4	-0.050	-0.035	-0.024
C_5	0.010	0.009	0.007
C_6	-0.063	-0.041	-0.026
C_7/α_{em}	-0.020	-0.004	0.019
C_8/α_{em}	0.082	0.052	0.033
C_9/α_{em}	-1.339	-1.263	-1.201
C_{10}/α_{em}	0.369	0.253	0.168
$C_{7\gamma}$	-0.341	-0.304	-0.272
C_{8g}	-0.160	-0.145	-0.132

of the operators [4]. So the derivation of the effective Hamiltonian can be called "the first step factorization".

Several years ago, the perturbative corrections to the Wilson coefficients in SM have been evaluated to next-to-leading order with renormalization group method. We list their numerical results in the naive dimensional regularization (NDR) scheme and at the three scales $m_b/2$, m_b and $2m_b$ in Table 1.

2.2 QCD Factorization in the Heavy Quark Limit

After "first step factorization", the decay amplitude for $B \to P_1 P_2$ can be written as

$$\mathcal{A}(B \to P_1 P_2) = \sum_i v_i C_i(\mu) \langle P_1 P_2 | Q_i(\mu) | B \rangle . \tag{4}$$

The central task now is to reliably evaluate the transition matrix element $\langle P_1P_2|Q_i(\mu)|B\rangle$. Note that the matrix element contains two scales: $\mathcal{O}(m_b)$ and Λ_{QCD} , it is hoped that $\langle P_1P_2|Q_i(\mu)|B\rangle$ can be separated into short-distance contributions which relate to large scale $\mathcal{O}(m_b)$ and long-distance contributions that relate to Λ_{QCD} . Then short-distance contributions which are perturbatively calculable should recover the scheme and scale dependence of the hadronic matrix elements. And long-distance contributions can be parameterized by some universal non-perturbative parameters.

In Ref.[13], Beneke, Buchalla, Neubert and Sachrajda show that this idea of factorization can be realized, at least at one-loop order, in the heavy quark limit. They argue that the emitted meson P_1 carries large energy and momentum (about $m_B/2$) and therefore can be described by leading-twist light-cone distribution amplitudes. It is natural to imagine that the soft gluons would decouple from the emitted P_1 at leading order of Λ_{QCD}/m_b since the $q\bar{q}$ pair in P_1 form a small-size color dipole. However, the factorization requires that not only soft divergences, but also collinear divergences should be

canceled. Fortunately, calculations at one-loop order explicitly show that, in the heavy quark limit, all infrared divergences vanish after summing over the four vertex correction diagrams (Figs. 1(a)-(d)). As to the recoiled meson P_2 , because the spectator quark in B meson is transferred to it as a soft parton, Beneke *et al.* believe that, instead of light-cone distribution amplitudes, one should use non-perturbative form factors F^{BP_2} to describe it. Light-cone sum rules also justify this non-perturbative property for the B to light form factors. It should be noted that when the spectator quark interacts with one of the quarks in the emitted meson by a hard gluon exchange, the recoiled meson can be described by leading-twist distribution amplitudes. These hard spectator diagrams (Figures 1(g)-(h)) can also be accounted for at the leading power of Λ_{QCD}/m_b . In summary, their factorization formula can be explicitly expressed as

$$\langle P_{1}P_{2}|Q_{i}|B\rangle = F^{B\to P_{2}}(0) \int_{0}^{1} dx T_{i}^{I}(x) \Phi_{P_{1}}(x) + \int_{0}^{1} d\xi dx dy T_{i}^{II}(\xi, x, y) \Phi_{B}(\xi) \Phi_{P_{1}}(x) \Phi_{P_{2}}(y)$$

$$= \langle P_{1}P_{2}|J_{1} \otimes J_{2}|B\rangle \cdot [1 + \sum r_{n}\alpha_{s}^{n} + \mathcal{O}(\Lambda_{QCD}/m_{b})]. \tag{5}$$

We call this factorization formalism as QCD factorization or the BBNS approach. In the above formula, $\Phi_B(\xi)$ and $\Phi_{P_i}(x)$ (i=1,2) are the leading-twist wave functions of B and the light pseudoscalar mesons respectively, and the $T_i^{I,II}$ denote hard-scattering kernels which are calculable in perturbation theory. At the order of α_s , the hard kernels $T^{I,II}$ can be depicted by Fig. 1. Figures 1(a)-1(d) represent vertex corrections, Figs. 1(e) and 1(f) penguin corrections, and Figs. 1(g) and 1(h) hard spectator scattering.

Comparing this approach with "naive factorization" and/or "generalized factorization", there are some interesting characteristics:

- (i) At the leading order of α_s , it can reproduce the results of "naive factorization", at the higher order of α_s , the renormalization scheme and scale dependence for the hadronic matrix elements can be recovered from the hard-scattering kernels T_i^I . The "generalized factorization" can also obtain the necessary dependence on scheme and scale. However, this dependence is the results of one loop calculations of quark-level matrix elements. According to Buras et al., quark-level matrix elements are accompanied by infrared divergences. To avoid these divergences, one usually assume that external quark states are off-shell. Unfortunately, it will introduce gauge dependence which is also unphysical. In Ref. [12], the authors give a calculation assuming the external quarks are on-shell, and they show that the infrared singularities can be canceled by assuming the final quarks are in the form of hadrons, then their calculation is gauge independent. Their idea is almost the same as the BBNS approach. The differences is: in the BBNS approach, the ejected meson is represented as its light-cone distribution amplitude; in Ref.[12], the constraint for the ejected $q\bar{q}$ pair is that it is a color-singlet object and the quark and the anti-quark have almost the same momentum. Because results in Ref. [12] are still from a calculation at quark level, some information from the distributions of momentum fraction in hadrons are ignored.
- (ii) "Generalized factorization" considers non-factorizable contributions as intractable. Therefore, one may introduce one or more effective color numbers N_c^{eff} to phenomenologically represent non-factorizable contributions. Furthermore, N_c^{eff} is assumed to be universal to maintain predictive power. However, QCD factorization tells us that "non-factorizable" contributions is indeed factorizable and therefore calculable in the heavy

quark limit. In consequence, N_c^{eff} can be calculated which is process-dependent beyond leading order of α_s .

- (iii) A particular interesting result of QCD factorization is that strong phases come solely from hard scattering processes and are therefore calculable in the heavy quark limit. From Eq.(5), it is easy to conclude that the imaginary part of decay amplitude arises only from hard scattering kernels T_i^I because non-perturbative form factors and light-cone distribution amplitudes are all real. T_i^I contains vertex corrections (Figs. 1 (a)-(d)) and penguin corrections (Figure 1(e)-(f)). Strong phases from penguin corrections are commonly called by the Bander-Silverman-Soni (BSS) mechanism[24], which is the unique source of strong phases in "generalized factorization". However, the gluon virtuality of Figure 1(e), which is well defined in QCD factorization, is ambiguous in "generalized factorization" and usually treated as a free parameter. In addition, vertex corrections will also contribute to strong phases in QCD factorization, which is missed in the "generalized factorization".
- (iv) Hard spectator contributions (Figure 1(g)-(h)), which is leading power effects in QCD factorization, are missing in "naive factorization" and "generalized factorization". The readers can be referred to ref [13, 18] for more details.

2.3 Chirally Enhanced Corrections in QCD Factorization

It is observed that QCD factorization is demonstrated only in the strict heavy quark limit. This means that any generalization of QCD factorization to include or partly include power corrections of Λ_{QCD}/m_b should re-demonstrate the factorization. There are a variety of sources which may contribute to power corrections in $1/m_b$, examples are higher twist distribution amplitudes, transverse momenta of quarks in the light meson, annihilation diagrams etc.. Unfortunately, there is no known systematic way to evaluate these power corrections in general for exclusive decays. Moreover, factorization might break down when these power corrections, for instance transverse momenta effects, are considered. This indicates that one might have to give up such an ambitious plan that all power corrections could be, at least in principle, incorporated into QCD factorization order by order. One might argue that power corrections in B decays are numerically unimportant because these corrections are proportional to a small number $\Lambda_{QCD}/m_b \simeq 1/15$. But it is not true. For instance, the contributions of operator Q_6 to decay amplitudes would formally vanish in the strict heavy quark limit. However it is numerically very important in penguin-dominant B rare decays, such as interesting channels $B \to \pi K$ etc.. This is because Q_6 is always multiplied by a formally power suppressed but chirally enhanced factor $r_{\chi} = \frac{2m_P^2}{m_b(m_1+m_2)} \sim \mathcal{O}(1)$, where m_1 and m_2 are current quark masses. So power suppression might probably fail at least in this case. Therefore phenomenological applicability of QCD factorization in B rare decays requires at least a consistent inclusion of chirally enhanced corrections.

Chirally enhanced corrections arise from twist-3 light-cone distribution amplitudes, generally called $\phi_p(x)$ and $\phi_{\sigma}(x)$. For light pseudoscalar mesons, they are defined as [26]

$$\langle P(p')|\bar{q}(y)i\gamma_5 q(x)|0\rangle = f_P \mu_P \int_0^1 du \ e^{i(up'\cdot y + \bar{u}p'\cdot x)} \phi_p(u), \tag{6}$$

$$\langle P(p')|\bar{q}(y)\sigma_{\mu\nu}\gamma_{5}q(x)|0\rangle = if_{P}\mu_{P}(p'_{\mu}z_{\nu} - p'_{\nu}z_{\mu})\int_{0}^{1}du \ e^{i(up'\cdot y + \bar{u}p'\cdot x)}\frac{\phi_{\sigma}(u)}{6}, \qquad (7)$$

where $\mu_p = \frac{m_p^2}{m_1 + m_2}$, z = y - x, m_1 and m_2 are the corresponding current quark masses. So when chirally enhanced corrections are concerned, the final light mesons should be described by leading twist and twist-3 distribution amplitudes [27]

$$\langle P(p')|\bar{q}_{\alpha}(y)q_{\delta}(x)|0\rangle = \frac{if_{P}}{4} \int_{0}^{1} du \ e^{i(up'\cdot y+\bar{u}p'\cdot x)} \times \left\{ p'\gamma_{5}\phi(u) - \mu_{P}\gamma_{5} \left(\phi_{p}(u) - \sigma_{\mu\nu}p'^{\mu}z^{\nu}\frac{\phi_{\sigma}(u)}{6}\right) \right\}_{\delta\alpha}.$$
(8)

Then it is crucial to show that factorization really holds when considering twist-3 distribution amplitudes. The most difficult part is to demonstrate the infrared finiteness of the hard scattering kernels T_i^I . For more technical details of this proof, the readers are referred to the literature [15, 16].

With these effective operators, $B \to P_1 P_2$ decay amplitudes in QCD factorization can be written as

$$A(B \to P_1 P_2) = \frac{G_F}{\sqrt{2}} \sum_{p=u,c} \sum_{i=1}^{n} v_p a_i^p \langle P_1 P_2 | Q_i | B \rangle_F, \tag{9}$$

where v_p is CKM factor, $\langle P_1 P_2 | Q_i | B \rangle_F$ is the factorized matrix element and is the same as the definition of the BSW Largrangian[5]. And the explicit expressions for the decay amplitudes of $B \to P_1 P_2$ are listed in the appendix of [11, 12].

Then as an illustration, the explicit expressions of a_i^p (i=1 to 10) for $B \to \pi\pi$ (using symmetric LCDAs of the pion) are obtained. But it is easy to generalize these formulas to the case that the final states are other light pseudoscalars. Furthermore, we take only part of QED corrections into account in our final formula, in particular the QED penguin insertions. Now a_i^p for $B \to \pi\pi$ in NDR γ_5 scheme is listed as follows:

$$a_1^u = C_1 + \frac{C_2}{N} + \frac{\alpha_s}{4\pi} \frac{C_F}{N} C_2 F,$$
 (10)

$$a_2^u = C_2 + \frac{C_1}{N} + \frac{\alpha_s}{4\pi} \frac{C_F}{N} C_1 F, \tag{11}$$

$$a_3 = C_3 + \frac{C_4}{N} + \frac{\alpha_s}{4\pi} \frac{C_F}{N} C_4 F, \tag{12}$$

$$a_4^p = C_4 + \frac{C_3}{N} + \frac{\alpha_s}{4\pi} \frac{C_F}{N} C_3 F$$

$$-\frac{\alpha_s}{4\pi} \frac{C_F}{N} \left\{ C_1 \left(\frac{4}{3} \log \frac{\mu}{m_b} + G(s_p) - \frac{2}{3} \right) + \left(C_3 - \frac{C_9}{2} \right) \left(\frac{8}{3} \log \frac{\mu}{m_b} + G(0) + G(1) - \frac{4}{3} \right) + \sum_{q=u,d,s,c,b} \left(C_4 + C_6 + \frac{3}{2} e_q C_8 + \frac{3}{2} e_q C_{10} \right) \left(\frac{4}{3} \log \frac{\mu}{m_b} + G(s_q) \right) + G_8 C_{8G} \right\},$$
(13)

$$a_{5} = C_{5} + \frac{C_{6}}{N} + \frac{\alpha_{s}}{4\pi} \frac{C_{F}}{N} C_{6}(-F - 12),$$

$$a_{6}^{p} = C_{6} + \frac{C_{5}}{N} - \frac{\alpha_{s}}{4\pi} \frac{C_{F}}{N} 6C_{5}$$

$$-\frac{\alpha_{s}}{4\pi} \frac{C_{F}}{N} \left\{ C_{1}((1 + \frac{2}{3}A_{\sigma}) \log \frac{\mu}{m_{b}} - \frac{1}{2} - \frac{1}{3}A_{\sigma} + G'(s_{p}) + G^{\sigma}(s_{p})) + \sum_{\sigma=d,b} (C_{3} - \frac{C_{9}}{2})((1 + \frac{2}{3}A_{\sigma}) \log \frac{\mu}{m_{b}} - \frac{1}{2} - \frac{1}{3}A_{\sigma} + G'(s_{q}) + G^{\sigma}(s_{q})) \right\}$$

$$(14)$$

$$+ \sum_{q=u,d,s,c,b} (C_4 + C_6 + \frac{3}{2} e_q C_8 + \frac{3}{2} e_q C_{10}) \left((1 + \frac{2}{3} A_{\sigma}) \log \frac{\mu}{m_b} + G'(s_q) + G^{\sigma}(s_q) \right)$$

$$+ (\frac{3}{2} + A_{\sigma}) C_{8G} \right\},$$

$$(15)$$

$$a_7 = C_7 + \frac{C_8}{N} + \frac{\alpha_s}{4\pi} \frac{C_F}{N} C_8 (-F - 12),$$

$$a_8^p = C_8 + \frac{C_7}{N} - \frac{\alpha_s}{4\pi} \frac{C_F}{N} 6C_7$$

$$- \frac{\alpha_{em}}{9\pi} \left\{ (C_2 + \frac{C_1}{N}) ((1 + \frac{2}{3} A_{\sigma}) \log \frac{\mu}{m_b} - \frac{1}{2} - \frac{1}{3} A_{\sigma} + G'(s_p) + G^{\sigma}(s_p)) \right.$$

$$+ (C_4 + \frac{C_3}{N}) \sum_{q=d,b} \frac{3}{2} e_q ((1 + \frac{2}{3} A_{\sigma}) \log \frac{\mu}{m_b} - \frac{1}{2} - \frac{1}{3} A_{\sigma} + G'(s_q) + G^{\sigma}(s_q))$$

$$+ (C_3 + \frac{C_4}{N} + C_5 + \frac{C_6}{N}) \sum_{q=u,d,s,c,b} \frac{3}{2} e_q \left((1 + \frac{2}{3} A_{\sigma}) \log \frac{\mu}{m_b} + G'(s_q) + G^{\sigma}(s_q) \right)$$

$$+ (\frac{3}{4} + \frac{1}{2} A_{\sigma}) C_{7\gamma} \right\},$$

$$(17)$$

$$a_9 = C_9 + \frac{C_{10}}{N} + \frac{\alpha_s}{4\pi} \frac{C_F}{N} C_{10} F,$$

$$a_{10}^p = C_{10} + \frac{C_9}{N} + \frac{\alpha_s}{4\pi} \frac{C_F}{N} C_{10} F,$$

$$+ (C_4 + \frac{C_3}{N}) \sum_{q=d,b} \frac{3}{2} e_q (\frac{4}{3} \log \frac{\mu}{m_b} + G(s_q) - \frac{2}{3})$$

$$+ (C_3 + \frac{C_4}{N} + C_5 + \frac{C_6}{N}) \sum_{q=d,s} \frac{3}{2} e_q (\frac{4}{3} \log \frac{\mu}{m_b} + G(s_q)) + \frac{1}{2} C_8 C_{7\gamma} \right\}.$$

$$(19)$$

Here N=3 is the number of color, $C_F=(N^2-1)/2N$ is the factor of color, $s_q=m_q^2/m_b^2$ and we define the other symbols in the above expressions as

$$F = -12\ln\frac{\mu}{m_b} - 18 + f^I + f^{II},\tag{20}$$

$$f^{I} = \int_{0}^{1} dx \ g(x)\phi(x), \ G_{8} = \int_{0}^{1} dx \ G_{8}(x)\phi(x), \tag{21}$$

$$G(s) = \int_{0}^{1} dx \ G(s, x)\phi(x),$$
 (22)

$$G'(s) = \int_{0}^{1} dx \ G'(s, x)\phi_{p}(x), \tag{23}$$

$$G^{\sigma}(s) = \int_{0}^{1} dx \ G^{\sigma}(s, x) \frac{\phi_{\sigma}(x)}{6(1 - x)}, \qquad A_{\sigma} = \int_{0}^{1} dx \ \frac{\phi_{\sigma}(x)}{6(1 - x)}, \tag{24}$$

where $\phi(x)$ [$\phi_p(x)$, $\phi_{\sigma}(x)$] is leading twist (twist-3) LCDA of the ejected pion, and the hard-scattering functions are

$$g(x) = 3\frac{1-2x}{1-x}\ln x - 3i\pi, \quad G_8(x) = \frac{2}{1-x},\tag{25}$$

$$G(s,x) = -4 \int_{0}^{1} du \ u(1-u) \ln(s - u(1-u)(1-x) - i\epsilon), \tag{26}$$

$$G'(s,x) = -3 \int_{0}^{1} du \ u(1-u) \ln(s - u(1-u)(1-x) - i\epsilon), \tag{27}$$

$$G^{\sigma}(s,x) = -2\int_{0}^{1} du \ u(1-u)\ln(s-u(1-u)(1-x)-i\epsilon)$$

$$+ \int_{0}^{1} du \frac{u^{2}(1-u)^{2}(1-x)}{s-u(1-u)(1-x)-i\epsilon}.$$
 (28)

The contributions from the hard spectator scattering [Figs. 1(g), 1(h)] are reduced to the factor f^{II} :

$$f^{II} = \frac{4\pi^2}{N} \frac{f_{\pi} f_B}{F_{+}^{B \to \pi}(0) m_B^2} \int_0^1 d\xi \, \frac{\Phi_B(\xi)}{\xi} \int_0^1 dx \, \frac{\phi(x)}{x} \int_0^1 dy \, \left[\frac{\phi(y)}{1 - y} + \frac{2\mu_{\pi}}{M_B} \frac{\phi_{\sigma}(y)}{6(1 - y)^2} \right]. \tag{29}$$

There contains a divergent integral in f^{II} . When we do numerical calculation in this work, we will simply parameterize this divergence as what done by Beneke *et al.*[14]:

$$\int (dy/y) = \ln(m_b/\Lambda_{QCD}) + \varrho e^{i\phi}, \qquad (30)$$

where ϕ is an arbitrary phase, $0^{\circ} \le \phi \le 360^{\circ}$, and ϱ is varied from 0 to 3 (realistic) or 6 (conservative).

We illustrate numerically the scale dependence of a_i^p in Table 2. Here we use the asymptotic form of the LCDAs of the light pseudoscalar meson which are

$$\phi(x) = 6x(1-x), \tag{31}$$

$$\phi_p(x) = 1, \tag{32}$$

$$\phi_{\sigma}(x) = 6x(1-x), \tag{33}$$

and we set $f^{II} = 0$ in computation because of its large uncertainty.

From the expressions and numerical results of the coefficients a_i , some general observations are listed below:

1. We have shown that the coefficients a_i (i = 1 - 5, 7, 9, 10) are renormalization scale independent at order of α_s with asymptotic LCDAs in [15],

$$\frac{\mathbf{d}a_i}{\mathbf{d}\ln\mu} = 0 \qquad (i \neq 6, 8),$$

¹This parameterization is a little bit different from that in recent paper[16] by Beneke et al., but the variation of these two parameterization are almost the same. In addition, we have pointed out in [15] that f^{II} might be convergent if the transverse momentum k_T of the parton is taken into account, furthermore, the Sudakov resummation might be also considered. In Ref.[28], the authors find that value of f^{II} is really in the range of the above parameterization when the Sudakov suppression is taken into account. In recent literature[29] of PQCD method, the authors point out that the threshold resummation can also help to suppress the singularities at the endpoints, especially for the twist-3 level.

Table 2: Numerical values of coefficients a_i with $m_b = 4.6$ GeV, $m_c = 1.45$ GeV and $f^{II} = 0$.

	$\mu = m_b/2$	$\mu = m_b$	$\mu = 2m_b$
a_1^u	1.070 + 0.026i	1.046 + 0.013i	1.027 + 0.006i
a_2^u	-0.019-0.106i	0.023- 0.079 i	$0.062 \text{-} 0.064 \mathrm{i}$
$a_3(10^{-4})$	93.662+46.585i	73.837+25.729i	51.675+14.646i
$a_4^u(10^{-4})$	-330.78-179.23i	-297.17 -146.84i	-267.83 -125.46i
$a_4^c(10^{-4})$	-403.19-55.903i	-351.48-54.337i	-311.41 -51.226i
$a_5(10^{-4})$	-98.679-58.697i	-67.453-30.139i	-41.612 -15.867i
$a_6^u(10^{-4})$	-556.39-159.84i	-411.61-136.65i	-322.84 -120.02i
$a_6^c(10^{-4})$	-597.2-34.652i	-442.22-42.742i	-347.41 -44.663i
$a_6^u r_{\chi}(10^{-4})$	-474.17-136.22i	-469.29-155.8 i	-459.82-170.95i
$a_6^c r_{\chi}(10^{-4})$	-508.95-29.531i	-504.19-48.731i	-494.81-63.614i
$a_7(10^{-4})$	0.458 + 0.597i	1.248 + 0.299i	2.591 + 0.157i
$a_8^u(10^{-4})$	6.980-0.66i	4.255 - 1.117i	2.336 - 1.465i
$a_8^c(10^{-4})$	6.884-0.365i	4.076- 0.566 i	2.092 - 0.717i
$a_8^u r_\chi(10^{-4})$	5.949-0.562i	4.852 - 1.274i	3.328-2.087i
$a_9(10^{-4})$	-97.902-2.686i	-94.935-1.453i	-91.732-0.801i
$a_{10}^u(10^{-4})$	7.414 + 9.087i	3.136 + 6.136i	-0.956 + 4.261i
$a_{10}^c(10^{-4})$	7.244 + 9.377i	2.817 + 6.679i	-1.389 + 4.998i

However, a_6 and a_8 must be scale-dependent because that the factorized matrix elements multiplied by a_6 and a_8 are scale-dependent. But,

$$\frac{\mathbf{d}(a_i r_{\chi})}{\mathbf{d} \ln \mu} = 0 \qquad (i = 6, 8).$$

This point can also be seen roughly from numerical result in Table 2. It should be noted that the imaginary part of a_i is at the order of α_s , and its remaining scale dependence must be canceled by the radiative corrections from higher order of α_s .

- 2. The coefficients a_i are gauge independent. At the leading power of Λ_{QCD}/m_b , the light meson is represented as its leading twist light-cone wave function (LCWF). In the calculation, the Dirac structure of the leading twist LCWF guarantees that the light meson can be taken as a pair of collinear on-shell massless quark and antiquark. Therefore, the on-shell condition guarantees the gauge independence of a_i ($i \neq 6, 8$). In Ref.[16], the authors have shown that at the twist-3 level the light meson can be also taken as a pair of on-shell massless quark and anti-quark when the asymptotic form of twist-3 LCDAs are taken. Then, $a_{6,8}$ are also free of the gauge dependence.
- 3. The quantities of a_1 , a_2 receive a special attention, because they are related to tree operators $Q_{1,2}$, so, they are numerically large. QCD penguins effects are incorporated to the coefficients a_{3-6} , in which $a_{3,5}$ are smaller than $a_{4,6}$, and $a_3 + a_5$ is $\mathcal{O}(10^{-4})$. $a_{4,6}$ have the same order as a_2 , so they will play a dominant role when the

effects of tree operators are CKM-suppressed, for example in $b \rightarrow s$ transition. The electroweak penguin coefficients a_7 - a_{10} are even smaller. a_9 is the largest among them, and it can be comparable with the QCD penguin coefficients $a_{3,5}$. Thus, a_9 may play an important role in some decay modes, such as $B \rightarrow \pi^0 K$.

4. The imaginary part of a_i arises from the radiative corrections. Different from the "generalized factorization", the imaginary part of a_i comes not only from the penguin corrections (BSS mechanism), but also from the vertex corrections. However, it is suppressed by α_s , and generally numerically small. Thus, the strong phases evaluated from the BBNS approach are generally small. But in some special cases, the situation will be different. For example, the imaginary parts of $a_{2,4,6}$, especially for a_2 , are larger than those of other coefficients, so, when their contributions are dominant in some decay modes, strong interactions phases might be large, which would result in a large CP violation.

2.4 Contributions of Annihilation Amplitudes

Annihilation contributions appear in almost all charmless decay modes $B \to PP$. In some cases, they may be important in spite of the power suppression. As emphasized in PQCD method[30, 31], the weak annihilation can give a large imaginary part to the decay amplitudes. Then, within the frame of PQCD method, the large CP violations are expected. In this work, we will follow what have been done by Beneke et al.[16], writing the annihilation contributions in terms of convolutions of "hard-scattering" kernels with LCDAs by ignoring the soft endpoint divergences. This kind of treatment is obviously not self-consistent, however, it can help us to give an estimation of the annihilation. The corresponding diagrams of the weak annihilation are depicted in Figure 2. Here, we will follow the convention in Ref.[16].

$$\mathcal{A}^{ann} \Big(B \to P_1 P_2 \Big) \propto f_B f_{P_1} f_{P_2} \sum v_i \ r \ b_i$$
 (34)

The decay amplitudes of weak annihilation for $B \to PP$ are listed in the appendix. Then, we will apply the above formulae to revisit rare B decays in what follows.

3 Input Parameters

The decay amplitude for $B \rightarrow PP$ can be expressed by various parameters, such as: the CKM matrix elements, form factors, Wilson coefficients $C_i(\mu)$, LCDAs and so on. The values of these parameters will affect our predictions on CP-averaged branching ratios and CP-violating asymmetries. Now we will specify them for the use in calculation.

3.1 CKM Matrix Elements

CKM matrix in the Wolfenstein parameterization is read as:

$$V_{CKM} = \begin{pmatrix} 1 - \lambda^2/2 & \lambda & A\lambda^3(\rho - i\eta) \\ -\lambda & 1 - \lambda^2/2 & A\lambda^2 \\ A\lambda^3(1 - \rho - i\eta) & -A\lambda^2 & 1 \end{pmatrix} + \mathcal{O}(\lambda^4). \tag{35}$$

Here we take the Wolfenstein parameters from the fit of Ciuchini et al. [32]: $A=0.819\pm0.040$, $\lambda=0.2237\pm0.0033$, $\overline{\rho}=\rho(1-\lambda^2/2)=0.224\pm0.038$, $\overline{\eta}=\eta(1-\lambda^2/2)=0.317\pm0.040$ and $\gamma=(54.8\pm6.2)^\circ$. Correspondingly, we have $\rho=0.230\pm0.039$, $\eta=0.325\pm0.039$, and $\sqrt{\rho^2+\eta^2}=0.398\pm0.040$. If not stated otherwise, we shall use the central values as the default values.

3.2 Form Factors and Decay constants

Decay constants and heavy-to-light form factors are defined by following current matrix elements:

$$\langle P(q)|\bar{q}_1\gamma_\mu\gamma_5q_2|0\rangle = -if_Pq_\mu, \tag{36}$$

$$\langle P(q)|\bar{q}\gamma_{\mu}b|B\rangle = \left[(p+q)_{\mu} - \frac{m_B^2 - m_P^2}{(p-q)^2} (p-q)_{\mu} \right] F_1((p-q)^2) + \frac{m_B^2 - m_P^2}{(p-q)^2} (p-q)_{\mu} F_0((p-q^2)).$$
(37)

For decay constants we use $f_{\pi} = 131$ MeV, $f_{K} = 160$ MeV, $f_{B} = 180 \pm 40$ MeV. As to the decay constants related to the η and η' , we shall take the convention in [11, 12]:

$$\langle 0|\bar{q}\gamma^{\mu}\gamma_5 q|\eta^{(\prime)}(p)\rangle = i f_{\eta^{(\prime)}}^q p^{\mu},$$

and

$$\langle 0|\bar{s}\gamma_5 s|\eta^{(\prime)}(p)\rangle = -i\frac{(f_{\eta^{(\prime)}}^s - f_{\eta^{(\prime)}}^u)m_{\eta^{(\prime)}}^2}{2m_s}$$

$$\langle 0|\bar{u}\gamma_5 u|\eta^{(\prime)}(p)\rangle = \langle 0|\bar{d}\gamma_5 d|\eta^{(\prime)}(p)\rangle = \frac{f_{\eta^{(\prime)}}^u}{f_{\eta^{(\prime)}}^s} \langle 0|\bar{s}\gamma_5 s|\eta^{(\prime)}(p)\rangle.$$

Here we shall not consider the charm quark content in $\eta^{(\prime)}$. The relations between η - η' mixing and η_8 - η_0 (the SU(3)-octet and -singlet) are:

$$|\eta\rangle = \cos\theta_8|\eta_8\rangle - \sin\theta_0|\eta_0\rangle, \qquad |\eta'\rangle = \sin\theta_8|\eta_8\rangle + \cos\theta_0|\eta_0\rangle,$$
 (38)

$$f_{\eta}^{u} = \frac{f_{8}}{\sqrt{6}}\cos\theta_{8} - \frac{f_{0}}{\sqrt{3}}\sin\theta_{0}, \qquad f_{\eta'}^{u} = \frac{f_{8}}{\sqrt{6}}\sin\theta_{8} + \frac{f_{0}}{\sqrt{3}}\cos\theta_{0},$$
 (39)

$$f_{\eta}^{s} = -2\frac{f_{8}}{\sqrt{6}}\cos\theta_{8} - \frac{f_{0}}{\sqrt{3}}\sin\theta_{0}, \qquad f_{\eta'}^{s} = -2\frac{f_{8}}{\sqrt{6}}\sin\theta_{8} + \frac{f_{0}}{\sqrt{3}}\cos\theta_{0}, \tag{40}$$

Here f_8 , f_0 are decay constants of η_8 , η_0 respectively, θ_8 , θ_0 are the mixing angles. Their values are [33]: $f_8 \approx 1.28 f_{\pi} \approx 168 \text{ MeV}$, $f_0 \approx 1.20 f_{\pi} \approx 157 \text{ MeV}$, $\theta_8 \approx -22.2^{\circ}$, $\theta_0 \approx -9.1^{\circ}$. We take $F_0^{B\pi} = 0.28 \pm 0.05$ which is obtained by light-cone sum rule [10]. For $B \rightarrow K$, $\eta^{(\prime)}$ transitions, the following relations are applied to give their corresponding values:

$$\frac{f_{\pi}}{f_{K}} \approx \frac{F_{0}^{B\pi}(0)}{F_{0}^{BK}(0)}, \quad F_{0,1}^{B\eta} = F_{0,1}^{B\pi} \left(\frac{\cos\theta_{8}}{\sqrt{6}} - \frac{\sin\theta_{0}}{\sqrt{3}}\right), \quad F_{0,1}^{B\eta'} = F_{0,1}^{B\pi} \left(\frac{\sin\theta_{8}}{\sqrt{6}} + \frac{\cos\theta_{0}}{\sqrt{3}}\right). \tag{41}$$

3.3 Quark Masses

There are two types of quark mass in our analysis. One type is the pole mass which appears in the loop-integration. Accompanied with the α_s order corrections to the hadronic matrix elements, they contribute to coefficients a_i through the functions G(s, x), G'(s, x) and $G^{\sigma}(s, x)$, or G(s), G'(s) and $G^{\sigma}(s)$. Here we fix them as:

$$m_u = m_d = m_s = 0$$
, $m_c = 1.45 \text{GeV}$, $m_b = 4.6 \text{GeV}$.

The other type quark mass appears in the hadronic matrix elements and the chirally enhanced factor r_{χ} through equations of motion. They are renormalization scale-dependent. And their values have been summarized in [34]. Here we shall use the PDG2000 data for discussion:

$$\overline{m}_b(\overline{m}_b) = 4.0 \sim 4.4 \text{GeV}, \quad \overline{m}_s(2GeV) = 75 \sim 170 \text{MeV},$$

 $\overline{m}_d(2GeV) = 3 \sim 9 \text{MeV}, \quad \overline{m}_u(2GeV) = 1 \sim 5 \text{MeV}.$

Here, for b quark and s quark, we take their central values as default values. Because the current masses of light quarks are difficult to fix, we would like to take

$$r_{\eta^{(\prime)}} \left(1 - \frac{f_{\eta^{(\prime)}}^u}{f_{\eta^{(\prime)}}^s}\right) = r_{\pi} = r_K = r_{\chi}.$$

We think that it is a good approximation in our calculation. Using the renormalization group equation, we can get the corresponding running r_{χ} at the scale $\mu = \mathcal{O}(m_b)$:

$$r_{\chi}(m_b/2) = 0.85, \quad r_{\chi}(m_b) = 1.14, \quad r_{\chi}(2m_b) = 1.42.$$

4 Numerical Analysis

4.1 Branching ratios and comparison with data

In the B mesons rest frame, we have two-body decay width

$$\Gamma(B \to P_1 P_2) = \frac{1}{8\pi} \frac{|p|}{m_B^2} |\mathcal{A}(B \to P_1 P_2)|^2, \tag{42}$$

where

$$|p| = \frac{\sqrt{\left[m_B^2 - (m_{P_1} + m_{P_2})^2\right] \left[m_B^2 - (m_{P_1} - m_{P_2})^2\right]}}{2m_B}.$$

The corresponding branching ratio is

$$\mathcal{B}r(B \to P_1 P_2) = \frac{\Gamma(B \to P_1 P_2)}{\Gamma_{tot}},\tag{43}$$

where $\tau = 1/\Gamma_{tot}$. In our calculation, we take $\tau = 1.548 \times 10^{-12}$ sec for B^0 , and $\tau = 1.653 \times 10^{-12}$ sec for B^{\pm} . In addition, because we work in the heavy quark limit, we take the mass of light meson as zero in the computation of phase space, then $|p| = m_B/2$.

We show experimental data and theoretical predictions on the CP-averaged branching ratios for $B\rightarrow PP$ in Table 3 and Table 4 respectively. In Table 4, we give the averages of the branching ratios of $B\rightarrow PP$ and their CP-conjugate modes with the default values of parameters at three different renormalization scales $\mu=m_b/2$, m_b , $2m_b$. From Table 3 and Table 4 some remarks are in order:

Table 3: Experimental data of CP-averaged branching ratios for $B \rightarrow \pi\pi$, πK , $K\eta'$ in unit of 10^{-6} .

Decay Mode	CLEO [1]	BaBar [2]	Belle [3]
$\overline{B}^0 \rightarrow \pi^+\pi^-$	$4.3^{+1.6}_{-1.4}\pm0.5$	$4.1 \pm 1.0 \pm 0.7$	$5.6^{+2.3}_{-2.0} \pm 0.4$
$B^{\pm}{\to}\pi^{\pm}\pi^{0}$	$5.6^{+2.6}_{-2.3}\pm 1.7$	$5.1^{+2.0}_{-1.8} \pm 0.8$	$7.8^{+3.8+0.8}_{-3.2-1.2}$
$\overline{B}^0 {\to} \pi^{\pm} K^{\mp}$	$17.2^{+2.5}_{-2.4}\pm1.2$	$16.7 \pm 1.6 \pm 1.3$	$19.3^{+3.4+1.5}_{-3.2-0.6}$
$B^{\pm}{ ightarrow}\pi^0K^{\pm}$	$11.6^{+3.0+1.4}_{-2.7-1.3}$	$10.8^{+2.1}_{-1.9}\pm1.0$	$16.3^{+3.5+1.6}_{-3.3-1.8}$
$B^{\pm} \rightarrow \pi^{\pm} K^0$	$18.2^{+4.6}_{-4.0} \pm 1.6$	$18.2^{+3.3}_{-3.0} \pm 1.7$	$13.7^{+5.7+1.9}_{-4.8-1.8}$
$\overline{B}^0 {\to} \pi^0 \overline{K}^0$	$14.6^{+5.9}_{-5.1}^{+2.4}_{-3.3}$	$8.2^{+3.1}_{-2.7}\pm1.1$	$16.0^{+7.2+2.5}_{-5.9-2.7}$
$B^-{ ightarrow} K^-\eta'$	$80^{+10}_{-9}\pm7$	$70 \pm 8 \pm 5$	$79^{+12}_{-11} \pm 9$
$\overline{B}^0 \rightarrow \overline{K}^0 \eta'$	$89^{+18}_{-16} \pm 9$	$42^{+13}_{-11} \pm 4$	$55^{+19}_{-16} \pm 8$

1. For the decay modes $B \to \pi\pi$ and $B \to \pi K$, our predictions are consistent with those by Beneke et al. [16]. In these modes, with the default values of the parameters, we find that the CP-averaged branching ratios of $B^{\pm} \to \pi^0 \pi^-$ (\simeq pure tree) and $B^{\pm} \to K^0 \pi^{\pm}$ (pure penguin) are in good agreement with the experimental measurements. Therefore these two decay modes can be considered as good probes of QCD factorization for B meson decays to two light mesons [36]. For the other modes $B \to \pi\pi$ and $B \to \pi K$, the predictions of the CP-averaged branching ratios by using the default values of the parameters seem not very good comparing with the experimental measurements. In particular, the theoretical prediction for the branching ratio of $B^0 \to \pi^+\pi^-$ is larger than the experimental data. The same situation also occurs in the "generalized factorization" [11, 12]. For the other decays modes $B \to \pi K$, our predictions seem smaller than the measurements. But taking the uncertainties of the input parameters into account, such as the CKM matrix elements (especially the angle γ and $|V_{ub}|$), the endpoint divergences in hard spectator scattering and weak annihilations, form factors etc., it is possible that the theoretical predictions by the BBNS approach can be in accord with the experimental results. For instance, when $\mu = m_b$, $\gamma = 150^{\circ}$, theoretical predictions for $B^0 \to \pi^+ \pi^-$, $\pi^+ K^-$ and $B^- \to \pi^0 K^-$ will be in accord with experiments,

$$\mathcal{B}r^{f}(\overline{B}^{0} \to \pi^{+}\pi^{-}) = 4.87 \times 10^{-6}, \qquad \mathcal{B}r^{f+a}(\overline{B}^{0} \to \pi^{+}\pi^{-}) = 5.09 \times 10^{-6},$$

$$\mathcal{B}r^{f}(\overline{B}^{0} \to \pi^{+}K^{-}) = 15.77 \times 10^{-6}, \quad \mathcal{B}r^{f+a}(\overline{B}^{0} \to \pi^{+}K^{-}) = 16.08 \times 10^{-6},$$

$$\mathcal{B}r^{f}(B^{-} \to \pi^{0}K^{-}) = 11.11 \times 10^{-6}, \quad \mathcal{B}r^{f+a}(B^{-} \to \pi^{0}K^{-}) = 11.25 \times 10^{-6},$$
(44)

where $\mathcal{B}r^f$ and $\mathcal{B}r^{f+a}$ are the predictions of the CP-averaged branching ratios by QCD factorization without and with considering the weak annihilation respectively. We will illustrate this point in next subsection in detail.

2. We note that experimental data for CP-averaged branching ratios for $B \rightarrow K \eta'$ are about 4 times larger than our theoretical predictions with default values of the parameters, likewise the results under GF framework [11, 12]. In Refs.[11, 12], the charm quark content in η' is considered, however, this mechanism cannot give a good

Table 4: Numerical predictions for CP-averaged branching ratios (in unit of 10^{-6}) for $B \rightarrow PP$, under framework of NF and QCDF, where $\mathcal{B}r^f$ and $\mathcal{B}r^{f+a}$ denote the CP-averaged branching ratio without and with considering the contributions from the weak annihilation respectively. The experimental data is from PDG2000, * denotes uncorrelate averages of Table 3, ** denotes upper limits given by [3], † denotes upper limits in [2].

		$\mu = m_b/$			$\mu = m_b$					
decay	NF		CDF	NF		CDF	NF		CDF	Exp.
modes	$\mathcal{B}r$	$\mathcal{B}r^f$	$\mathcal{B}r^{f+a}$	$\mathcal{B}r$	$\mathcal{B}r^f$	$\mathcal{B}r^{f+a}$	$\mathcal{B}r$	$\mathcal{B}r^f$	$\mathcal{B}r^{f+a}$	
$\overline{B}^0 \rightarrow \pi^+ \pi^-$	9.74	10.06	10.49	9.09	9.67	9.97	8.68	9.36	9.58	$4.4{\pm}0.9^*$
$B^-{\rightarrow}\pi^-\pi^0$	5.58	5.26	_	6.20	5.36	_	6.76	5.52	_	$5.7{\pm}1.5^*$
$B^-{ ightarrow}\pi^-\eta$	3.41	3.27	3.22	3.59	3.28	3.26	3.74	3.34	3.33	< 15
$B^- \rightarrow \pi^- \eta'$	2.26	2.23	2.18	2.53	2.26	2.24	2.71	2.35	2.34	< 12**
$\overline{B}^0 \rightarrow \pi^0 \eta$	0.17	0.17	0.18	0.12	0.15	0.16	0.07	0.14	0.15	< 8
$\overline{B}^0 \rightarrow \pi^0 \eta'$	0.038	0.048	0.054	0.037	0.045	0.053	0.026	0.049	0.057	< 11
$\overline{B}^0 \rightarrow \pi^0 \pi^0$	0.12	0.11	0.18	0.15	0.099	0.13	0.23	0.10	0.12	< 9.3
$\overline{B}^0 \rightarrow \eta \eta$	0.077	0.078	0.092	0.095	0.076	0.087	0.12	0.081	0.089	< 18
$\overline{B}^0 \rightarrow \eta' \eta'$	0.009	0.016	0.014	0.029	0.015	0.017	0.048	0.021	0.024	< 47
$\overline{B}^0 \rightarrow \eta \eta'$	0.059	0.073	0.081	0.11	0.073	0.082	0.15	0.086	0.096	< 27
$\overline{B}^0 \rightarrow K^- \pi^+$	10.66	9.56	10.45	6.40	8.59	9.13	3.4	7.78	8.09	$17.4 \pm 1.5^*$
$\overline{B}^0 \rightarrow \overline{K}^0 \pi^0$	4.99	4.52	4.96	2.90	4.01	4.27	1.44	3.57	3.72	$10.3\pm2.6^*$
$B^- \rightarrow K^- \pi^0$	7.65	7.04	7.56	4.83	6.36	6.67	2.82	5.78	5.96	$12.1 \pm 1.6^*$
$B^- \rightarrow \overline{K}^0 \pi^-$	14.43	13.45	14.48	8.8	11.99	12.61	4.79	10.72	11.08	$17.3 \pm 2.5^*$
$B^-{ ightarrow} K^-\eta$	2.91	2.67	2.78	1.68	2.31	2.37	0.94	1.96	2.0	< 14
$B^-{\rightarrow}K^-\eta'$	16.6	16.72	17.82	12.47	15.74	16.87	7.49	15.75	16.55	$74.9 \pm 6.6^*$
$\overline{B}^0 \rightarrow \overline{K}^0 \eta$	1.93	1.70	1.79	1.0	1.45	1.50	0.45	1.21	1.24	< 33
$\overline{B}^0 \rightarrow \overline{K}^0 \eta'$	17.07	17.33	18.13	12.82	16.26	17.12	7.79	16.14	16.73	$59.6 \pm 9.8^*$
$B^- \rightarrow K^- K^0$	0.78	0.75	0.79	0.47	0.67	0.69	0.26	0.59	0.61	$<2.5^{\dagger}$
$\overline{B}^0 \rightarrow \overline{K}^0 K^0$	0.73	0.71	0.84	0.44	0.62	0.70	0.24	0.56	0.60	< 17
$\overline{B}^0 {\to} K^+ K^-$	—	_	0.044	_	_	0.033		_	0.03	$< 2.5^{\dagger}$

explanation for experimental data yet. The unexpected large data have triggered considerable theoretical interest in understanding the mechanism of η' production, and have been widely discussed in the literature[35]. So far, it is generally assumed that di-gluon fusion mechanism could enhance η' production, but the shape of form factor of the vertex $g^*g^*\eta'$ bring a very large uncertainty to predict the contribution from di-gluon mechanism [37]. Recently, M.Z. Yang and Y.D. Yang give a calculation for $B \to \eta^{(\prime)}P$ within the frame of BBNS approach [21], in which the di-gluon mechanism is considered. In that paper, the author give a consistent calculation for the vertex of $g^*g^*\eta'$ in the perturbative QCD, and find the branching ratios of $B \to K\eta'$ are really enhanced and in agreement with the experimental measurement.

3. For the decays $B^{\pm} \to \pi^{\pm} \eta^{(\prime)}$, $K^{\pm} \eta$, the CP-averaged branching ratios predicted by the BBNS approach are at the order of 10^{-6} . We expect that these decay modes can be observed soon at BaBar and Belle².

²Recently, Belle and BaBar collaborations report their measurements of the branching ratio of the

- 4. The decays $B^0 \to \pi^0 \pi^0$, $\pi^0 \eta^{(\prime)}$, $\eta^{(\prime)} \eta^{(\prime)}$, our predictions shows that their CP-averaged branching ratios are very small and about $\mathcal{O}(10^{-7}) \sim \mathcal{O}(10^{-8})$. If these predictions are reliable, it is very difficult to observe these decay modes at BaBar and Belle.
- 5. In the BBNS approach, the predictions for the branching ratios of $B \to KK$ are highly suppressed, especially for $B^0 \to K^+K^-$ which is purely from the weak annihilation contributions. In Ref.[38], the authors gave an estimation for the decays $B \to KK$ using the PQCD method, and also found that their branching ratios are very small. These decay modes can be a good probe for the long distance final state interaction (FSI). On other hand, from the Appendix, if endpoint divergence X_A is universal, the measurement for the branching ratio of $B^0 \to K^+K^-$ may give a constraint for the range of X_A .

In Table 4, for a comparison, we also give the estimations for the CP-averaged branching ratios of $B \to PP$ using the naive factorization (NF) approximation. Again, we list the predictions by the BBNS approach with and without considering the weak annihilation together. From these results, some general observations are given as follows:

- Obviously, predictions on branching ratios for $B \rightarrow PP$ using BBNS approach are less scale-dependent compared with those under NF framework, especially in $b \rightarrow s$ transition, such as $B \rightarrow K\pi$, $K\eta^{(\prime)}$. Noting that a_i are calculated at one-loop level, if the corrections from high order of α_s were taken into account, the scale-dependence of theoretical predictions might be further reduced.
- Generally, the contributions from weak annihilation are highly power suppressed. However, due to the endpoint divergence, they may give observable contributions in our results. In $B \to \pi K$, we can see that the weak annihilation can give about $5\% \sim 10\%$ enhancement. Note that the results of Table 4 are computed by the default parameters. If we varied the parameters for the endpoint divergences in weak annihilations, it will bring much larger uncertainties to our predictions. This will be shown in the next subsection in details.

4.2 Uncertainty of Predictions

In Figure 3, based on the BBNS approach, we show the dependence of branching ratios for $B \to \pi\pi$, πK and $K\eta'$ on weak phase γ , scanning all ranges of variation of parameters, including CKM matrix elements, form factors, endpoint divergence $\int_0^1 dx/x$ and so on. Note that weak annihilation effects do not contribute to $B^{\pm} \to \pi^{\pm}\pi^{0}$. We can see that our theoretical predictions give very wide dot-shades for the branching ratios within the range of parameters, so predictions for CP-averaged branching ratios of $B \to \pi\pi$, πK , $K\eta'$ are consistent with the experimental data if we select appropriate parameters.

In Figure 4, we show the dependence of the CP-averaged branching ratios of $B^0 \to \pi^0 K^0$, $B^\pm \to K^\pm \pi^0$ and $B^0 \to \pi^+ \pi^-$ on the CKM matrix elements, form factors, endpoint divergence in hard spectator scattering and weak annihilations. From Figure 4, some remarks are given in order.

decay $B^{\pm} \to \pi^{\pm} \eta'$ which is consistent with zero. The 90% CL upper limit is $\mathcal{B}r(B^{\pm} \to \pi^{\pm} \eta') < 7 \times 10^{-6}$ (at Belle) or $\mathcal{B}r(B^{\pm} \to \pi^{\pm} \eta') < 12 \times 10^{-6}$.

• For the decays $B^0 \to \pi^0 K^0$ and $B^{\pm} \to K^{\pm} \pi^0$, the CP-averaged branching ratios weakly depend on $|V_{ub}/V_{cb}|$ because that the decays $B \to \pi K$ are dominated by penguin diagrams and $|v_u/v_c| = |(V_{us}^* V_{ub})/(V_{cs}^* V_{cb})|$ is highly suppressed by $\mathcal{O}(\lambda^2)$ in $b \to s$ transition. For the case of $B^0 \to \pi^+ \pi^-$, though it is a tree-dominant $(b \to u)$ process, the penguin pollution plays an important role. For illustration, the decay amplitude of $\bar{B}^0 \to \pi^+ \pi^-$ reads

$$\mathcal{A}(\bar{B}^0 \to \pi^+ \pi^-) = -i \frac{G_F}{\sqrt{2}} f_{\pi} F^{B\pi}(0) m_B^2 \Big\{ v_u \Big[a_1 + a_4^u + a_{10}^u + \Big(a_6^u + a_8^u \Big) r_{\chi} \Big] + v_c \Big[a_4^c + a_{10}^c + \Big(a_6^c + a_8^c \Big) r_{\chi} \Big] \Big\}.$$

$$(45)$$

Note that $|v_u| = |V_{ud}^* V_{ub}|$ is at the same order as $|v_c| = |V_{cd}^* V_{cb}|$ and $|(a_4 + a_6 r_\chi)/a_1| \sim 0.1$, so the branching ratio of $\bar{B}^0 \to \pi^+ \pi^-$ is sensitive to both of $|V_{ub}/V_{cb}|$ and $\gamma = \arg(V_{ub}^*)$. (In contrast, the decay amplitude of $B^{\pm} \to \pi^0 \pi^{\pm}$ suffers less pollution from the penguin contribution which is proportional to the small electroweak penguin coefficient $a_9 + a_{10} - a_7 + a_8 r_\chi$.) Therefore, the variation of $|V_{ub}/V_{cb}|$ brings large uncertainty to the prediction for the branching ratio of $B^0 \to \pi^+ \pi^-$.

- All the three modes are dominated by the form factor $F^{B\pi}(0)$. Varying $F^{B\pi}(0)$ from 0.23 to 0.33, it takes about $\pm 35\%$ uncertainty to the branching ratios. By using the ratios of the branching ratios, the uncertainties brought by the form factor can be largely reduced. This will be shown later.
- The endpoint divergence in the hard spectator scattering does not bring large uncertainty to our predictions. The reason is that the endpoint divergence only contains a single logarithmic term and its coefficient is suppressed by α_s and the color number N.
- Obviously, the endpoint divergence in weak annihilation brings large uncertainty, in particular, to the decays $B \to \pi K$. In Ref.[16], the authors also showed this point of view. The reason is that the endpoint divergence in weak annihilation is dominated by a product of two logarithmic terms. Within the range of the parameters ϱ and φ , our predictions by BBNS approach are in agreement with the experimental measurements.

Therefore, we find that the weak annihilation is the main source of the uncertainties in the BBNS approach. To obtain more precise prediction, it needs further analysis on the weak annihilations. Furthermore, we also find that our prediction for the CP-averaged branching ratio of $\bar{B}_d^0 \to \pi^+\pi^-$ especially when $\gamma \geq 90^\circ$ seems still greater than the experimental measurement. Some researchers pointed out the elastic and inelastic long-distance FSI can help us obtain small branching ratio for $\bar{B}_d^0 \to \pi^+\pi^-$ at small $\gamma[41, 42]$. However, with the elastic FSI, in order to get the satisfying results, one must introduce a large stong phase difference which is unbelievable in the heavy quark limit. Particularly, in Ref.[42], the author takes the inelastic rescattering $B \to D\bar{D} \to \pi\pi$ into account and finds that the small branching ratio of $\bar{B}_d^0 \to \pi\pi$ can be obtained at the small γ without fine-tunning of the input parameters.

Here we emphasize that the decay amplitude of $B^0 \to K^-K^+$ comes completely from the effects of weak annihilations under BBNS approach, because contributions of weak

annihilations are supposed to be power suppressed, so CP-averaged branching ratio for $\overline{B}^0(B^0) \to K^+K^-$ is small in Figure 3. At the same time, we can also see that uncertainties of theoretical predictions for these decay modes are very large (the branching ratios range from 10^{-8} to 10^{-7}). As mentioned above, we expect that we can extract some useful information about the endpoint divergence $\int_0^1 dx 1/x$ from $B^0 \to K^+K^-$. However, the present experimental upper limit is much greater than our predictions within the range of the parameters. If this decay mode can be measured precisely in the future, then we will be able to obtain some useful information on weak annihilations and FSI, so that the endpoint divergence $\int_0^1 dx/x$ can be determined effectively.

4.3 Ratios of the Branching ratios

As mentioned above, the decay rates for $B \rightarrow PP$ depend on a number of parameters which the BBNS approach itself cannot predict, thus these parameters result in ambiguity of predictions on the CP-averaged branching ratios. In order to reduce uncertainties from the renormalization scale and weak annihilation effects etc. as much as possible, the ratios of CP-averaged branching ratios are good quantities. Furthermore, many methods have been suggested to give bounds on γ using decay modes of $B \rightarrow \pi\pi$, πK , in which the ratios of branching ratios play important roles. We hope that our calculation can give some constraint on γ . In Figure 5, we show some ratios of CP-averaged branching ratios versus the weak phase γ (note: we use PDG2000 data for $\tau_{B^+}/\tau_{B^0}=1.062$), where the slashed-line bands correspond to experimental data listed in Table 3 with one standard deviation (1σ) .

Obviously, using the ratios of branching ratios, and comparing with Figure 3, the width of dot-shades become narrow due to the reduction of the uncertainty. From Figure 5(b), the ratio $\frac{\mathcal{B}r(B^0 \to \pi^{\mp}K^{\pm})}{2\mathcal{B}r(B^0 \to \pi^0K^0)}$ is consistent with the experimental data at small $\gamma \leq 60^{\circ}$. However, the ratio $\frac{\tau_{B^+}}{\tau_{B^0}} \frac{\mathcal{B}r(B^0 \to \pi^+\pi^-)}{2\mathcal{B}r(B^0 \to \pi^{\pm}\pi^0)}$ set a limit $\gamma \geq 120^{\circ}$ in Figure 5(e). We can impose restrictions on the angle $60^{\circ} \leq \gamma \leq 180^{\circ}$ from Figure 5(a) and Figure 5(d), which are consistent with the results of [16]. In Ref.[16], the authors give a global fit for $(\bar{\rho}, \bar{\eta})$ from B rare hadronic decays using QCD factorization. The result prefers large γ and/or small $|V_{ub}|[16, 36]$.

There are many discussions on ratios of branching ratios, for instance in [11, 12], in order to determine coefficients a_i , and extract the CKM matrix parameters etc.. Especially decay modes $B \rightarrow K\pi$ are widely discussed to get information on γ , readers interested in these topics are referred to, for instance, [39, 40]. From Figures 5(a) and 5(b), our theoretical results show that

$$\frac{2\mathcal{B}r(B^{\pm}\to\pi^{0}K^{\pm})}{\mathcal{B}r(B^{\pm}\to\pi^{\pm}K^{0})} \approx \frac{\mathcal{B}r(B^{0}\to\pi^{\mp}K^{\pm})}{2\mathcal{B}r(B^{0}\to\pi^{0}K^{0})}$$
(46)

This approximate relation can be also obtained from the isospin decomposition of the effective Hamiltonian ¹ [43]. And, the experimental data listed in Table 3 give

$$\frac{2\mathcal{B}r(\pi^{0}K^{\pm})}{\mathcal{B}r(\pi^{\pm}K^{0})} = 1.18 \pm 0.34 (\text{BaBar}), \qquad \frac{\mathcal{B}r(\pi^{\mp}K^{\pm})}{2\mathcal{B}r(\pi^{0}K^{0})} = 1.02 \pm 0.41 (\text{BaBar}), \qquad (47)$$

which are consistent with Eq.(46).

¹In Ref.[43], the isospin amplitudes are defined as: $B_{1/2} = \sqrt{\frac{2}{3}} \langle \frac{1}{2}, \pm \frac{1}{2} | \mathcal{H}_{\Delta I=0} | \frac{1}{2}, \pm \frac{1}{2} \rangle$, which arises from

4.4 CP-violating asymmetries

CP violation in B meson decays can be either direct or indirect. Typically the direct CP-violating asymmetry arises when tree and penguin amplitudes interfere. CP violations in decays of charged B meson are purely direct, as these decays are all self-tagging, they are definitive signals of CP violation if seen. The direct CP-violating symmetry is defined by

$$\mathcal{A}_{CP} = \frac{\Gamma(B^- \to f^-) - \Gamma(B^+ \to f^+)}{\Gamma(B^- \to f^-) + \Gamma(B^+ \to f^+)},\tag{48}$$

Because flavor eigenstates \overline{B}^0 and B^0 mix due to weak interactions, direct and indirect CP violation occur simultaneously in neutral B meson decays, and time-dependent measurements of CP-violating asymmetries are needed.

$$\mathcal{A}_{CP}(t) = \frac{\Gamma(\overline{B}^0(t) \to \bar{f}) - \Gamma(B^0(t) \to f)}{\Gamma(\overline{B}^0(t) \to \bar{f}) + \Gamma(B^0(t) \to f)},\tag{49}$$

For $B^0 \to f$ (but $B^0 \not\to \bar{f}$) and $\overline{B}^0 \to \bar{f}$ (but $\overline{B}^0 \not\to f$), their CP-violating asymmetries are similar to those of charged B mesons. For $\overline{B}^0 \to (\bar{f} = f, CP|f) = \pm |f\rangle) \leftarrow B^0$, i.e. final states are CP eigenstates, the time-integrated CP-violating asymmetries are:

$$\mathcal{A}_{CP} = \frac{1}{1+x^2} a_{\epsilon'} + \frac{x}{1+x^2} a_{\epsilon+\epsilon'},\tag{50}$$

$$a_{\epsilon'} = \frac{1 - |\lambda_f|^2}{1 + |\lambda_f|^2}, \ a_{\epsilon + \epsilon'} = \frac{-2\operatorname{Im}(\lambda_f)}{1 + |\lambda_f|^2}, \ \lambda_f = \frac{V_{tb}^* V_{td}}{V_{tb} V_{td}^*} \frac{\langle f | \mathcal{H}_{eff} | \overline{B}^0 \rangle}{\langle f | \mathcal{H}_{eff} | B^0 \rangle}, \tag{51}$$

with PDG2000 data $x = \Delta m/\Gamma = 0.73 \pm 0.03$ for $B^0 - \overline{B}^0$ system. Here $a_{\epsilon'}$ and $a_{\epsilon + \epsilon'}$ are due to direct and mixing-induced CP violation, respectively.

Recent experimental measurements of CP-violating asymmetries \mathcal{A}_{CP} for $B \to \pi K$, $K\eta'$ and $a_{\epsilon'}$, $a_{\epsilon+\epsilon'}$ for $\bar{B}_d^0 \to \pi^+\pi^-$ are listed in Table 5. These results contain very large errors and they are consistent with zero. The precise measurements of the direct CP violation and time-dependent CP violation are strongly expected in the near future.

Theoretically, CP-violating asymmetries will not be very large with BBNS approach in principle, because the strong phases are suppressed by α_s or Λ_{QCD}/m_b . However, from Table 2 we know that $a_{2,4,6}$ have large imaginary part. When they are dominant in some decay modes, large CP violations are expected, for instance, in $\overline{B}^0(B^0) \to \pi^0 \pi^0$, $\pi^0 \eta^{(\prime)}$, $\eta^{(\prime)} \eta^{(\prime)}$.

With BBNS approach, CP-violating asymmetries depend on several variables, such as form factors, CKM parameters, scale μ and so on. Our investigation indicates that CP-violating asymmetries for all $B \rightarrow PP$ depend very weakly on form factors, the same conclusion can be obtained with GF approach. So we show results only with default values of form factors in the following calculations. As for dependence of CP-violating

QCD penguin operators. While $A_{1/2}=\pm\sqrt{\frac{2}{3}}\langle\frac{1}{2},\pm\frac{1}{2}|\mathcal{H}_{\Delta I=1}|\frac{1}{2},\pm\frac{1}{2}\rangle$, $A_{3/2}=\sqrt{\frac{1}{3}}\langle\frac{3}{2},\pm\frac{1}{2}|\mathcal{H}_{\Delta I=1}|\frac{1}{2},\pm\frac{1}{2}\rangle$, which include contributions from tree and electroweak operators. Moreover, $|B_{1/2}|\approx\mathcal{O}(10^{-3})$, $|A_{1/2}|\approx\mathcal{O}(10^{-5})$, and $|A_{3/2}|\approx\mathcal{O}(10^{-4})$. The decay amplitudes can be described as $\mathcal{A}(B^+\to\pi^+K^0)=A_{3/2}+A_{1/2}+B_{1/2}$, and $\sqrt{2}\mathcal{A}(B^+\to\pi^0K^+)=2A_{3/2}-A_{1/2}-B_{1/2}$. Neglecting effects of $A_{3/2}$ and $A_{1/2}$, we can get a good approximation (46).

Table 5: Experimental data of CP-violating asymmetries \mathcal{A}_{CP} for $B \to \pi K, K \eta'$ and $a_{\epsilon'}$ and $a_{\epsilon+\epsilon'}$ for \bar{B}_d^0 in unit of percent.

Decay Modes	CLEO	BaBar	Belle
$\overline{B}^0(B^0) {\to} \pi^{\pm} K^{\mp}$	-4 ± 16	$-7 \pm 8 \pm 2$	$4.4^{+18.6+1.8}_{-16.7-2.1}$
$B^{\pm}{\to}\pi^0K^{\pm}$	-29 ± 23	$0 \pm 18 \pm 4$	$-5.9^{+22.2+5.5}_{-19.6-1.7}$
$B^{\pm}{\to}\pi^{\pm}K^0$	18 ± 24	$-21 \pm 18 \pm 3$	$9.8^{+43.0+2.0}_{-34.3-6.3}$
$B^{\pm}{\to}K^{\pm}\eta'$	3 ± 12		$6\pm15\pm1$

$$a_{\epsilon'}(\bar{B}_d^0 \to \pi^+\pi^-)$$
 $a_{\epsilon+\epsilon'}(\bar{B}_d^0 \to \pi^+\pi^-)$
BaBar $-25^{+45}_{-47} \pm 14$ $3^{+53}_{-56} \pm 11$

asymmetries on scale μ , there are six decay modes $\overline{B}^0(B^0) \to \pi^0 \pi^0$, $\pi^0 \eta^{(\prime)}$, $\eta^{(\prime)} \eta^{(\prime)}$ to be singled out because they are strongly μ -dependent compared with other decay modes. In these six decay modes, a_2 is involved and not CKM-suppressed, and it is sensitive to renormalization scale. This point has been shown in Table 2. Especially, its imaginary part is larger than its real part, which might result in large CP violations in these decay modes as we show in Table 7. We also list CP-violating asymmetries versus weak phase γ in Table 8 and Table 9. The endpoint divergence can cause large theoretical uncertainties, its influence on CP-violating asymmetries is shown in Table 6.

Table 6: The dependence of CP-averaged branching ratio and CP asymmetries for $B^{\pm} \rightarrow K^{\pm} \pi^0$ on ϱ, ϕ in endpoint divergence $\int_0^1 dx/x$. $\mathcal{B}r^f$ and $\mathcal{B}r^{f+a}$ have the same meanings as in Table 4. \mathcal{A}_{CP}^f and \mathcal{A}_{CP}^{f+a} can be defined in a similar way. The results are calculated with default values of other parameters at $\mu = m_b$ using BBNS approach.

ρ	0	3				6			
$\phi(deg)$		0	90	180	270	0	90	180	270
$\mathcal{B}r^f(10^{-6})$	6.37	6.31	6.36	6.43	6.38	6.25	6.35	6.49	6.39
$\mathcal{B}r^{f+a}(10^{-6})$	7.51	11.8	6.75	6.43	6.18	21.3	4.63	7.89	3.48
$\mathcal{A}^f_{CP}(\%)$	8.28	8.45	7.15	8.11	9.40	8.63	6.02	7.94	10.5
$\mathcal{A}^{f+a}_{CP}(\%)$	7.24	5.15	14.2	8.11	1.47	3.32	29.5	6.81	-12.4

From Table 6 to Table 9, we can clearly see that theoretical predictions on CP-violating asymmetries are compatible with measurements within one standard deviation (1 σ). Unfortunately, the present experimental uncertainties are too large to draw any meaningful conclusion. In addition, weak annihilations have great influence on CP-violating asymmetries, so their contributions to decay amplitudes must be included in estimation of CP violation in B meson decays with BBNS approach. Moreover, the power corrections in order of Λ_{QCD}/m_b which are not included in the QCDF master formula (5). This needs further investigation.

Here we would like to point out that $B \rightarrow \pi\pi$ are usually considered to determine CKM

Table 7: The dependence of time-integrated CP-violating asymmetries $a_{\epsilon'}$, $a_{\epsilon+\epsilon'}$ and \mathcal{A}_{CP} (in unit of percent) for $\overline{B}^0(B^0) \to \pi^0 \pi^0$, $\pi^0 \eta^{(\prime)}$, $\eta^{(\prime)} \eta^{(\prime)}$ on renormalization scale μ , with the default values of various parameters and BBNS approach.

Decay Modes	scale μ	$a^f_{\epsilon'}$	$a_{\epsilon'}^{f+a}$	$a^f_{\epsilon+\epsilon'}$	$a_{\epsilon+\epsilon'}^{f+a}$	\mathcal{A}_{CP}^f	${\cal A}_{CP}^{f+a}$
_	$m_b/2$	-57.3	-69.3	-32.0	26.5	-52.6	-32.6
$\overline{B}^0(B^0) \rightarrow \pi^0 \pi^0$	m_b	-45.1	-79.0	-66.8	-12.4	-61.3	-57.4
	$2m_b$	-38.3	-82.4	-89.2	-46.3	-67.5	-75.8
_	$m_b/2$	35.5	62.7	9.72	-30.7	27.8	26.3
$\overline{B}^0(B^0) {\rightarrow} \pi^0 \eta$	m_b	31.5	63.3	12.2	-19.3	26.4	32.1
	$2m_b$	29.5	65.6	15.8	-9.75	26.8	38.1
	$m_b/2$	44.2	84.8	25.9	-35.3	41.2	38.5
$\overline{B}^0(B^0) \rightarrow \pi^0 \eta'$	m_b	41.8	81.0	19.6	-28.2	36.6	39.4
	$2m_b$	37.1	79.3	18.3	-17.4	33.0	43.5
_	$m_b/2$	55.5	46.6	58.8	56.9	64.2	57.5
$\overline{B}^0(B^0) { ightarrow} \eta \eta$	m_b	43.1	33.9	77.1	73.5	61.9	57.1
	$2m_b$	34.7	23.8	82.6	86.3	62.0	56.6
_	$m_b/2$	30.7	65.8	95.2	75.2	65.4	78.7
$\overline{B}^0(B^0) {\rightarrow} \eta' \eta'$	m_b	37.8	54.0	92.3	84.2	68.6	75.3
	$2m_b$	36.7	37.5	92.9	92.7	68.2	68.6
	$m_b/2$	55.6	56.8	74.1	65.1	71.5	68.1
$\overline{B}^0(B^0) {\to} \eta \eta'$	m_b	46.0	42.8	81.7	80.6	68.9	66.3
	$2m_b$	37.4	29.9	88.9	91.1	66.8	62.9

angle α and /or γ using CP-violating asymmetry [44, 45]. From Table 8 Table 9, we can see that $\mathcal{A}(\pi^+\pi^-)$, especially the mixing-induced $a_{\epsilon+\epsilon'}(\%)$ term, are sensitive to CKM angle γ , which are strongly polluted by penguins. As to large penguin pollution, recently R. Fleischer suggests a new approach [44]. Using U-spin SU(3) flavour symmetry, $B_d \rightarrow \pi^+\pi^-$ and $B_s \rightarrow K^+K^-$ are related to each other by interchanging d and s, which allow possibly a simultaneous determination β and γ . His analysis gives $\gamma = 76^{\circ}$ and $\phi_d = 2\beta = 53^{\circ}$ without considering U-spin-breaking effects.

As we see from Table 8 and Table 9, time-integrated CP-violating asymmetries \mathcal{A}_{CP} for $\overline{B}^0 \to K_S^0 \pi$, $K_S^0 \eta^{(\prime)}$ are completely dominated by mixing-induced $a_{\epsilon+\epsilon'}$ term. But we still do not know the $\eta^{(\prime)}$ production mechanism so far. Hence it is useless to mention about CP-violating asymmetries $\mathcal{A}_{CP}(K_S^0 \eta^{(\prime)})$. As to CP-violating asymmetries for $\overline{B}^0 \to K^+ K^-$, they do not contain direct CP-violating a'_{ϵ} term, and arise only from $a_{\epsilon+\epsilon'}$ term. Moreover they are sensitive to CKM angle γ . However, we know that with BBNS approach branching ratios for neutral B meson decays into $K^+ K^-$ have only weak annihilations contributions which are scale μ -dependent and contain large theoretical uncertainties due to their soft non-perturbative effects.

5 Conclusions

Table 8: CP-violating asymmetries $a_{\epsilon'}(\%)$ and $a_{\epsilon+\epsilon'}(\%)$ for neutral B meson decays with default values of various parameters using BBNS approach.

decay		$\gamma = 60^{\circ} \qquad \qquad \gamma = 90^{\circ} \qquad \qquad \gamma = 120^{\circ}$			$\gamma = 90^{\circ}$							
modes	$a^f_{\epsilon'}$	$a_{\epsilon'}^{f+a}$	$a^f_{\epsilon+\epsilon'}$	$a_{\epsilon+\epsilon'}^{f+a}$	$a^f_{\epsilon'}$	$a_{\epsilon'}^{f+a}$	$a^f_{\epsilon+\epsilon'}$	$a_{\epsilon+\epsilon'}^{f+a}$	$a^f_{\epsilon'}$	$a_{\epsilon'}^{f+a}$	$a^f_{\epsilon+\epsilon'}$	$a_{\epsilon+\epsilon'}^{f+a}$
$\pi^+\pi^-$	4.17	11.5	55.1	54.8	5.85	16.1	-30.7	-30.6	6.64	17.7	-92.0	-91.1
$\pi^0\eta$	31.2	60.8	11.4	-21.1	25.0	43.5	7.27	-22.1	16.6	27.3	4.21	-16.0
$\pi^0\eta'$	41.6	77.4	18.4	-31.8	34.7	54.5	11.5	-35.8	23.5	34.0	6.54	-26.3
$\pi^0\pi^0$	-41.5	-76.6	-65.3	-16.0	-25.6	- 56.9	-49.8	-23.7	-15.1	-36.4	-32.1	-18.8
$\eta\eta$	45.7	36.1	70.6	73.7	53.6	42.9	60.2	66.3	47.2	38.3	43.3	49.8
$\eta'\eta'$	41.7	58.8	89.7	80.8	65.7	83.8	65.3	53.4	89.9	94.6	38.4	26.3
$\eta\eta'$	49.7	46.1	81.0	80.2	65.5	59.6	68.8	70.1	66.1	58.7	50.7	52.8
$K_s^0 \pi^0$ $K_s^0 \eta$	1.78	2.37	77.0	76.6	2.14	2.83	74.1	73.7	1.92	2.54	58.8	58.3
$K_s^0 \eta$	3.08	3.62	77.8	77.4	3.72	4.36	75.1	74.7	3.38	3.95	59.9	59.3
$K_s^0 \eta'$	-1.92	-2.20	73.9	74.3	-2.25	-2.58	70.3	70.8	-1.97	-2.26	54.7	55.2
\overline{K}^0K^0	21.0	20.8	9.08	3.74	16.6	16.1	6.30	2.16	10.9	10.5	3.86	1.17
K^+K^-		0	_	72.9		0		3.47		0		-68.0

- 1. In the heavy quark limit, neglecting the effects of order Λ_{QCD}/m_b , the contributions which are non-factorizable under GF framework can be factorized with BBNS approach, and they are perturbatively calculable from first principle, at least at order of α_s . BBNS approach provides decay amplitudes with strong phases which are usually small, at order of α_s and/or Λ_{QCD}/m_b .
- 2. CP-averaged branching ratios of $B \rightarrow PP$ in BBNS approach are less renormalization scale-dependent comparing with those under NF framework, especially when the chirally enhanced corrections are taken into account; generally, with the appropriate parameters, predictions with BBNS approach are consistent with present experimental data. However, theoretical predictions include very large uncertainties which arise from various parameters, they suffer from influence of form factors, CKM matrix elements and soft endpoint divergence etc.. Our results show that theoretical uncertainties from the endpoint divergence $\int_0^1 dx/x$ are considerably large. Likewise, CP-violating asymmetries for $B \rightarrow PP$ in the BBNS approach are also sensitive to variation of endpoint divergences. Especially, decay amplitudes for $\overline{B}^0(B^0) \rightarrow K^+K^-$ arise completely from weak annihilations with the BBNS approach , we can obtain very useful informations on the effects of FSI and soft weak annihilations with precise experimental data in the future.
- 3. The present experimental data for non-leptonic B meson decays are not enough yet. Moreover their precision are not good enough, especially for the measurements of CP violation. On the other hand, there are still many uncertainties in the theoretical frame, for instance, the hard spectator scattering, weak annihilations and other potential power corrections. So it is too early to draw definite conclusions on CKM angles. The great advances in both experiment and theory in the near future are strongly expected.

Table 9: CP-violating asymmetries $\mathcal{A}_{CP}(\%)$ for decays of $B \rightarrow PP$ with default values of various parameters using BBNS approach.

decay	$\gamma = 60$		$\gamma =$		$\gamma = 120$		
modes	\mathcal{A}_{CP}^f	${\cal A}_{CP}^{f+a}$	\mathcal{A}_{CP}^f	${\cal A}_{CP}^{f+a}$	\mathcal{A}_{CP}^f	${\cal A}_{CP}^{f+a}$	
$\overline{B}^0(B^0) \rightarrow \pi^+\pi^-$	28.9	33.6	-10.8	-4.08	-39.6	-31.9	
$B^{\pm} \rightarrow \pi^{\pm} \pi^{0}$	0.07		0.09		0.08	—	
$B^{\pm} \rightarrow \pi^{\pm} \eta$	11.5	25.5	18.6	40.3	27.2	55.4	
$B^{\pm} \rightarrow \pi^{\pm} \eta'$	5.08	19.3	7.55	28.1	9.16	32.9	
$\overline{B}^0(B^0) {\rightarrow} \pi^0 \eta$	25.8	29.7	19.8	17.9	12.8	10.2	
$\overline{B}^0(B^0) {\rightarrow} \pi^0 \eta'$	35.9	35.4	28.1	18.5	18.5	9.60	
$\overline{B}^0(B^0) {\rightarrow} \pi^0 \pi^0$	58.1	57.6	40.4	48.4	25.2	32.7	
$\overline{B}^0(B^0) \rightarrow \eta \eta$	63.5	58.6	63.7	59.5	51.4	48.7	
$\overline{B}^0(B^0) \rightarrow \eta' \eta'$	69.9	76.9	74.0	80.1	76.9	74.3	
$\overline{B}^0(B^0) \rightarrow \eta \eta'$	71.0	68.3	75.5	72.3	67.3	63.4	
$\overline{B}^0(B^0) {\to} K^{\mp} \pi^{\pm}$	-6.53	-16.1	-5.91	-14.8	-4.20	-10.7	
$\overline{B}^0(B^0) {\rightarrow} K_S^0 \pi^0$	37.8	38.0	36.7	36.9	29.3	29.4	
$B^{\mp} \rightarrow K^{\mp} \pi^0$	-7.24	-15.0	-6.69	-14.1	-4.83	-10.3	
$B^{\mp} \rightarrow K_S^0 \pi^{\mp}$	-0.84	-1.05	-0.99	-1.24	-0.88	-1.10	
$B^{\mp} \rightarrow K^{\mp} \eta$	8.35	14.0	12.8	21.1	16.3	26.3	
$B^{\mp} \rightarrow K^{\mp} \eta'$	-3.19	-7.50	-3.41	-8.12	-2.75	-6.62	
$\overline{B}^0(B^0) {\rightarrow} K_S^0 \eta$	39.1	39.2	38.2	38.4	30.7	30.8	
$\overline{B}^0(B^0) {\rightarrow} K_S^0 \eta'$	34.0	33.9	32.0	32.0	24.8	24.8	
$B^{\mp} \rightarrow K^{\mp} K_S^0$	21.0	26.4	16.6	20.2	10.9	13.1	
$\overline{B}^0(B^0) \rightarrow \overline{K}^0K^0$	18.0	15.4	13.8	11.5	8.97	7.38	
$\overline{B}^0(B^0) {\rightarrow} K^+K^-$		34.7		1.65		-32.4	

Acknowledgements

This work is Supported in part by National Natural Science Foundation of China and State Commission of Science and Technology of China. We thank Profs. Zhi-zhong Xing and Mao-Zhi Yang for helpful discussions.

Appendix: The annihilation amplitudes for $B \rightarrow PP$

$$A^{ann}(\overline{B}^0 \to \pi^+ \pi^-) = -i \frac{G_F}{\sqrt{2}} f_B f_{\pi}^2 \left[v_u b_1 + (v_u + v_c) \left(b_3 + 2b_4 - \frac{1}{2} b_3^{ew} + \frac{1}{2} b_4^{ew} \right) \right], \quad (52)$$

$$A^{ann}(\overline{B}^0 \to \pi^0 \pi^0) = A^{ann}(\overline{B}^0 \to \pi^+ \pi^-), \tag{53}$$

$$A^{ann}(B^- \to \pi^0 \pi^-) = 0, (54)$$

$$A^{ann}(\overline{B}^0 \to \pi^0 \overline{K}^0) = i \frac{G_F}{2} f_B f_\pi f_K \left[(v_u + v_c) \left(b_3 - \frac{1}{2} b_3^{ew} \right) \right], \tag{55}$$

$$A^{ann}(\overline{B}^0 \to \pi^+ K^-) = -\sqrt{2}A^{ann}(\overline{B}^0 \to \pi^0 \overline{K}^0), \tag{56}$$

$$A^{ann}(B^{-} \to \pi^{0}K^{-}) = -i\frac{G_{F}}{2}f_{B}f_{\pi}f_{K}\left[v_{u}b_{2} + (v_{u} + v_{c})\left(b_{3} + b_{3}^{ew}\right)\right], \tag{57}$$

$$A^{ann}(B^- \to \pi^- \overline{K}^0) = \sqrt{2} A^{ann}(B^- \to \pi^0 K^-), \tag{58}$$

$$A^{ann}(\overline{B}^0 \to \pi^0 \eta^{(\prime)}) = -i \frac{G_F}{2} f_B f_\pi f_{\eta^{(\prime)}}^u \left[v_u 2b_1 + (v_u + v_c) \left(-2b_3 + b_3^{ew} + 3b_4^{ew} \right) \right], (59)$$

$$A^{ann}(B^{-} \to \pi^{-} \eta^{(\prime)}) = -i \frac{G_F}{\sqrt{2}} f_B f_{\pi} f_{\eta^{(\prime)}}^{u} \left[v_u 2b_2 + (v_u + v_c) \left(2b_3 + 2b_3^{ew} \right) \right], \tag{60}$$

$$A^{ann}(\overline{B}^0 \to \eta^{(\prime)}\eta^{(\prime)}) = -i\frac{G_F}{\sqrt{2}}f_B f_{\eta^{(\prime)}}^{u^2} \left[v_u 2b_1 + (v_u + v_c)\left(2b_3 + 4b_4 - b_3^{ew} + b_4^{ew}\right)\right], (61)$$

$$A^{ann}(\overline{B}^0 \to \eta \eta^{(\prime)}) = \frac{f_{\eta'}^u}{f_n^u} A^{ann}(\overline{B}^0 \to \eta \eta), \tag{62}$$

$$A^{ann}(B^{-} \to K^{-} \eta^{(\prime)}) = -i \frac{G_F}{\sqrt{2}} f_B f_K f_{\eta^{(\prime)}}^u \left(1 + \frac{f_{\eta^{(\prime)}}^s}{f_{\eta^{(\prime)}}^u} \right) \left[v_u b_2 + (v_u + v_c) \left(b_3 + b_3^{ew} \right) \right], \quad (63)$$

$$A^{ann}(\overline{B}^{0} \to \overline{K}^{0} \eta^{(\prime)}) = -i \frac{G_{F}}{\sqrt{2}} f_{B} f_{K} f_{\eta^{(\prime)}}^{u} \left(1 + \frac{f_{\eta^{(\prime)}}^{s}}{f_{\eta^{(\prime)}}^{u}} \right) \left[(v_{u} + v_{c}) \left(b_{3} - \frac{1}{2} b_{3}^{ew} \right) \right], \tag{64}$$

$$A^{ann}(\overline{B}^0 \to \overline{K}^0 K^0) = -i \frac{G_F}{\sqrt{2}} f_B f_K^2 \left[(v_u + v_c) \left(b_3 + 2b_4 - \frac{1}{2} b_3^{ew} - b_4^{ew} \right) \right], \tag{65}$$

$$A^{ann}(B^- \to K^- K^0) = -i \frac{G_F}{\sqrt{2}} f_B f_K^2 \left[v_u b_2 + (v_u + v_c) \left(b_3 + b_3^{ew} \right) \right], \tag{66}$$

$$A^{ann}(\overline{B}^0 \to K^+ K^-) = -i \frac{G_F}{\sqrt{2}} f_B f_K^2 \left[v_u b_1 + (v_u + v_c) \left(2b_4 + \frac{1}{2} b_4^{ew} \right) \right], \tag{67}$$

The annihilation coefficients (b_1, b_2) , (b_3, b_4) and (b_3^{ew}, b_4^{ew}) correspond to the contributions from tree, QCD penguins and electroweak penguins operators respectively. They are related to final state mesons. Using the asymmetry light cone distribution amplitudes of the mesons, and assuming SU(3) flavour symmetry, they can be expressed as [16]:

$$b_1 = \frac{C_F}{N_c^2} C_1 A^i, \qquad b_3 = \frac{C_F}{N_c^2} \Big[C_3 A^i + A^f \Big(C_5 + N_c C_6 \Big) \Big], \tag{68}$$

$$b_2 = \frac{C_F}{N_c^2} C_2 A^i, b_4 = \frac{C_F}{N_c^2} A^i (C_4 + C_6), (69)$$

$$b_3^{ew} = \frac{C_F}{N_c^2} \Big[C_9 A^i + A^f \Big(C_7 + N_c C_8 \Big) \Big], \tag{70}$$

$$b_4^{ew} = \frac{C_F}{N_c^2} A^i (C_{10} + C_8), (71)$$

and

$$A^{i} \approx \pi \alpha_{s} \left[18 \left(X_{A} - 4 + \frac{\pi^{2}}{3} \right) + 2r_{\chi}^{2} X_{A}^{2} \right]$$
 (72)

$$A^f \approx 12\pi\alpha_s r_\chi \left(2X_A^2 - X_A\right),\tag{73}$$

where $X_A = \int_0^1 \mathbf{dy}/y$ parameterizes the divergent endpoint integrals.

References

- [1] D. Cronin-Hennessy *et al.* (CLEO Collaboration), Phys. Rev. Lett. **85** 515 (2000); S.Chen *et al.* (CLEO Collaboration), Phys. Rev. Lett. **85** 525 (2000); S.J.Richichi et al. (CLEO Collaboration), Phys. Rev. Lett. **85** 520 (2000).
- [2] G. Cavoto (Babar Collaboration), hep-ex/0105018; B. Aubert *et al.* (Babar Collaboration), hep-ex/0105061, hep-ex/0107074, hep-ex/0108017; J. Olsen (Babar Collaboration), hep-ex/0011031.
- [3] T. Iijima (Belle Collaboration), hep-ex/0105005; K. Abe *et al.* (Belle Collaboration), hep-ex/0104030, hep-ex/0106095, hep-ex/0108010.
- [4] For a review, see G. Buchalla, A. J. Buras and M. E. Lautenbacher, Rev. Mod. Phys. **68** 1125 (1996); or A. J. Buras, hep-ph/9806471.
- [5] M. Bauer and B. Stech, Phys. Lett. B152 380 (1985); M.Bauer, B.Stech and M.Wirbel, Z. Phys. C34 (1987) 103.
- [6] J. D. Bjorken, Nucl. Phys. (Proc. Suppl.) **B11**, 325 (1989).
- [7] H. Y. Cheng, Phys .Lett. B335 428 (1994); Phys. Lett. B395 345 (1997); H. Y. Cheng and B. Tseng, Phys. Rev. D58 094005 (1998); A. Ali and C. Gerub, Phys. Rev. D57 2996 (1998); A. Ali, J. Chay, C. Gerub and P. Ko, Phys. Lett. B424 161 (1998); M. Neubert, Nucl. Phys. (Proc.Suppl.) B64 474 (1998); J. M. Soares, Phys. Rev. D51 3518 (1995).
- [8] A. Abada et al. (APE Collaboration), Phys. Lett. B365, 275 (1996); J.M. Flynn and C.T. Sachrajda, Heavy flavours II, 402-452, (hep-lat/9710057), J.M. Flynn et al. (UKQCD Collaboration), Nucl. Phys. B 461, 327 (1996); L. Del Debbio et al. (UKQCD Collaboration), Phys. Lett. B416, 392 (1998).
- [9] P. Ball and V. M. Braun, Phys. Rev. **D55**, 5561, (1997); J. High Energy Phys. **9809**, 005, (1998).
- [10] A. Khodjamirian, R. Rückl, S. Weinzierl and O. Yakovlev, Phys. Lett. B410, 275 (1997); A. Khodjamirian, R. Rückl and C.W. Winhart, Phys. Rev. D58, 054013 (1998); A. Khodjamirian, R. Rückl, Heavy flavours II, 345-401, (hep-ph/9801443); A. Khodjamirian, R. Rückl, S. Weinzierl, C.W. Winhart, O. Yakovlev, Phys. Rev. D62, 114002 (2000)
- [11] A.Ali, G.Kramer and C.D.Lü, Phys. Rev. D58 094009 (1998); Phys. Rev. D59 014005 (1999).
- [12] Y.H. Chen, H. Y. Cheng, B. Tseng and K.C. Yang, Phys. Rev. **D60**, 094014 (1999).
- [13] M. Beneke, G. Buchalla, M. Neubert and C. T. Sachrajda, Phys. Rev. Lett. 83, 1914 (1999).
- [14] M. Beneke, G. Buchalla, M. Neubert and C. T. Sachrajda, hep-ph/0007256.

- [15] D. S. Du, D. S. Yang and G. H. Zhu, hep-ph/0008216; Phys. Lett. B509, 263 (2001);
 Phys. Rev. D64, 014036 (2001).
- [16] M. Beneke, G. Buchalla, M. Neubert and C. T. Sachrajda, hep-ph/0104110.
- [17] J. Chay, Phys.Lett. **B476**, 339 (2000).
- [18] M. Beneke, G. Buchalla, M. Neubert and C. T. Sachrajda, Nucl. Phys. **B591**, 313 (2000).
- [19] D. S. Du, D.S. Yang and G.H. Zhu, Phys. Lett. **B488**, 46, (2000).
- [20] T. Muta, A. Sugamoto, M. Z. Yang and Y. D. Yang, Phys. Rev. **D62**, 094020 (2000).
- [21] M. Z. Yang and Y. D. Yang, Phys. Rev. **D62**, 114019 (2000); hep-ph/0012208.
- [22] X. G. He, J. P. Ma, C. Y. Wu, hep-ph/0008159.
- [23] J. Chay, C. Kim, hep-ph/0009244.
- [24] M. Bander, D. Silverman and A. Soni, Phys. Rev. Lett. 43, 242 (1979).
- [25] H.Y. Cheng and K.C. Yang, Phys. Rev. **D63**, 074011, (2001); hep-ph/0012152.
- [26] V. L. Chernyak and A. R. Zhitnitsky, Phys. Rep. 112, 173 (1983); V. M. Braun and I. B. Filyanov, Z. Phys.C48, 239 (1990); P. Ball, J. High Energy Phys. 9901, 010 (1999).
- [27] M. Beneke, hep-ph/0009328, submitted to J.Phys.G.
- [28] D. S. Du, C. S. Huang, Z. T. Wei and M. Z. Yang, hep-ph/0107320.
- [29] H. N. Li, hep-ph/0103305; T. Kurimoto, H. N. Li and A. I. Sanda, hep-ph/0105003.
- [30] Y. Y. Keum, H. N. Li, A. I. Sanda, Phys. Rev. D63, 054008 (2001); Phys. Lett. B504, 6 (2001).
- [31] C. D. Lü, K. Ukai and M. Z. Yang, Phys.Rev. **D63**, 074009 (2001).
- [32] M.Ciuchini *et al.*, hep-ph/0012308.
- [33] T. Feldmann, P. Kroll, B. Stech, Phys. Rev. **D58**, 114006 (1998).
- [34] P.Colangelo and A.Khodjamirian, [hep-ph/0010175].
- [35] D. S. Du, C. S. Kim and Y. D. Yang, Phys. Lett. B426, 133 (1998); A. L. Kagan and A. A. Petrov, hep-ph/9707354; A. L. Kagan, hep-ph/9806266; M. R. Ahmady, E. Kou and A. Sugamoto, Phys.Rev. D58, 014015 (1998).
- [36] M. Neubert, talk given in XX International Symposium on Lepton and Photon Interactions at High Energies (Roma, Italy, 23-28, July 2001).
- [37] D. S. Du, D. S. Yang and G. H. Zhu, hep-ph/9912201, to appear in High Energy Phys. and Nucl. Phys.

- [38] C. H. Chen, H. N. Li, Phys. Rev. **D63**, 014003 (2001).
- [39] M. Neubert and J. R. Rosner, Phys. Lett. **B441**, 403 (1998).
- [40] R. Fleischer and T. Mannel Phys. Rev. D57, 2757 (1998); A. J. Buras and R. Fleischer, Eur. Phys. J. C16, 97 (2000).
- [41] W.-S. Hou and K.-C. Yang, Phys. Rev. Lett. 84, 4806 (2000).
- [42] Z.-z Xing, Phys. Lett. **B493**, 301 (2000).
- [43] M. Neubert, Phys. Lett. **B424**, 152 (1998);
- [44] R. Fleischer, Eur. Phys. J C16, 87 (2000); hep-ph/0011323.
- [45] I. I. Bigi and A. I. Sanda, Nucl. Phys. B281, 41 (1987); Y. Nir and H. R. Quinn, Ann. Rev. Nucl. Part. Sci. 42, 211 (1992); P.Ball, hep-ph/0010024.

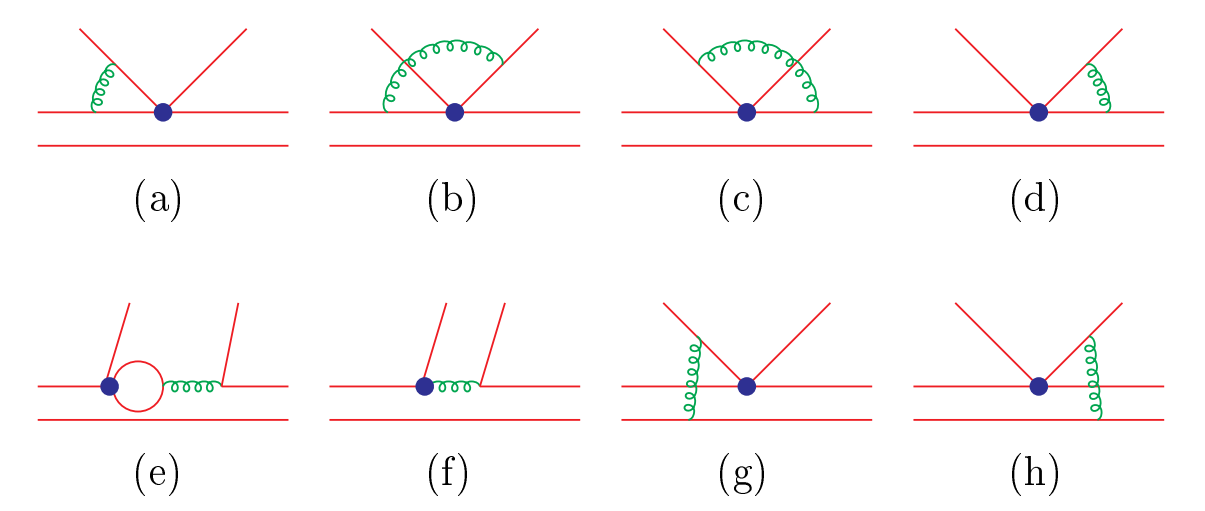


Figure 1: Order of α_s corrections to hard-scattering kernels. The upward quark lines represent the ejected light meson from b quark weak decays. These diagrams are commonly called vertex corrections, penguin corrections and hard spectator diagrams for Fig.(a)-(d), (e)-(f) and (g)-(h) respectively.

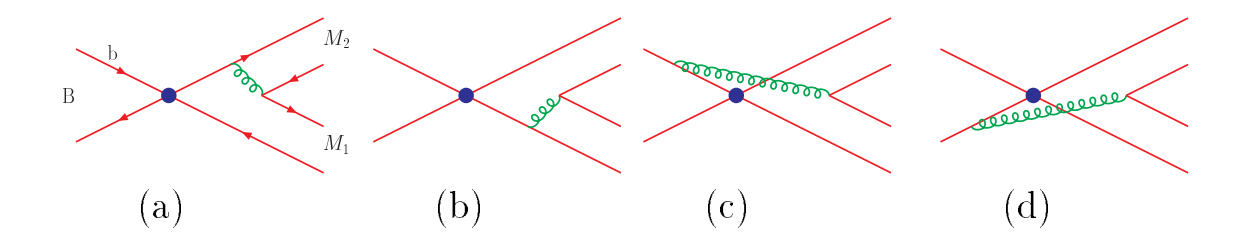


Figure 2: Order of α_s corrections to annihilation diagrams for $B{\to}PP$

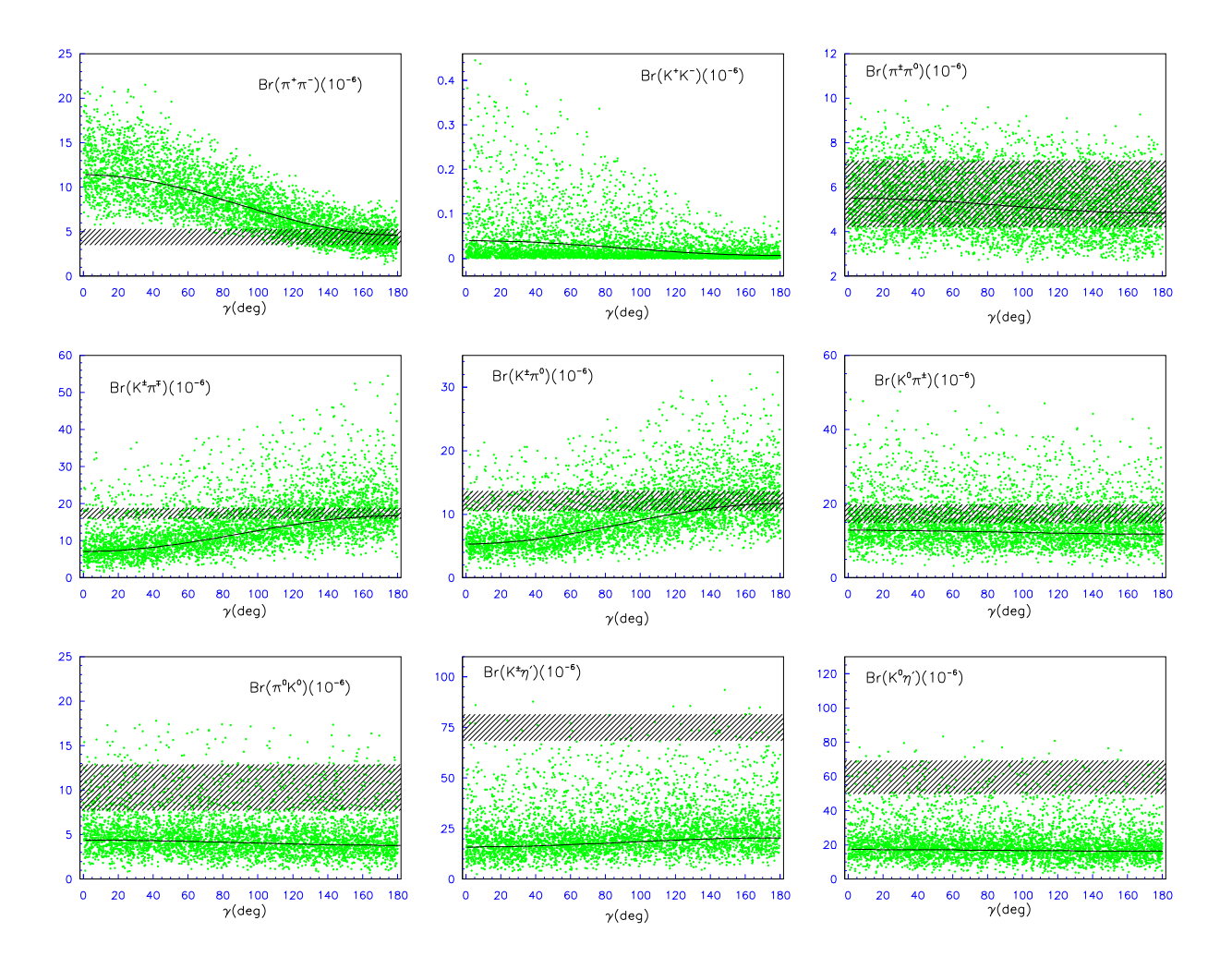


Figure 3: CP-averaged branching ratios as functions of γ . The solid lines are drawn with the default values at the scale of $\mu=m_b$, the horizontal slashed-line bands correspond to experimental data within one standard error, and the dot-shades denote the variation of the theory input parameters, including the CKM elements, the form factors, the uncertainty from weak annihilation and hard spectator scattering.

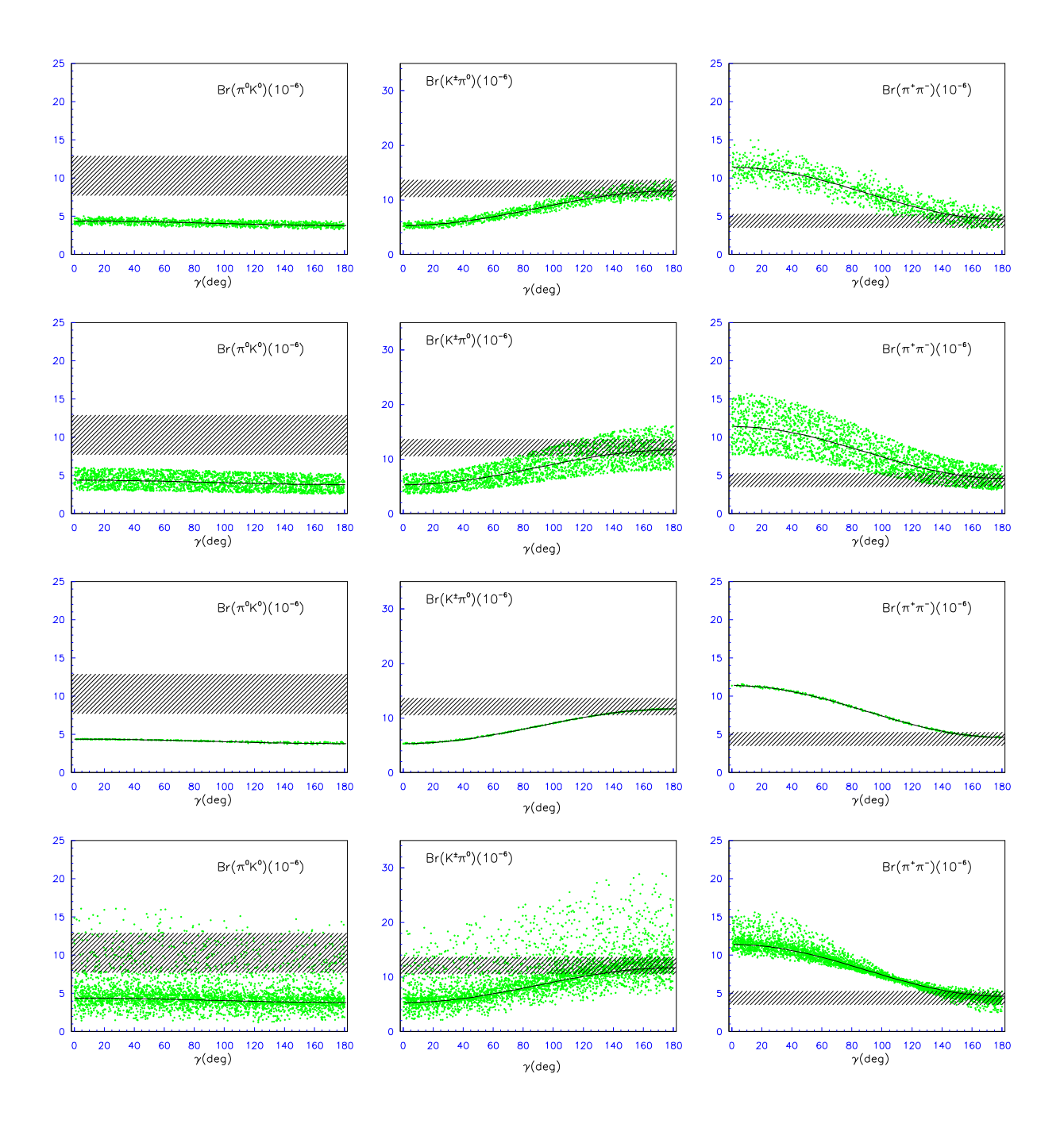


Figure 4: The dependence of CP-averaged branching ratios for $B^0 \to \pi^0 K^0$, $B^{\pm} \to K^{\pm} \pi^0$ and $B^0 \to \pi^+ \pi^-$ on the variations of input parameters under the QCDF approach at the renormalization scale $\mu = m_b$. The lines and bands have the same meaning as in Figure 3, and the dot-shades correspond to the variation of the CKM matrix elements especially $|V_{ub}|$ (the first row), form factors (the second row), endpoint divergences in the hard spectator scattering (the third row) and weak annihilations (the forth row).

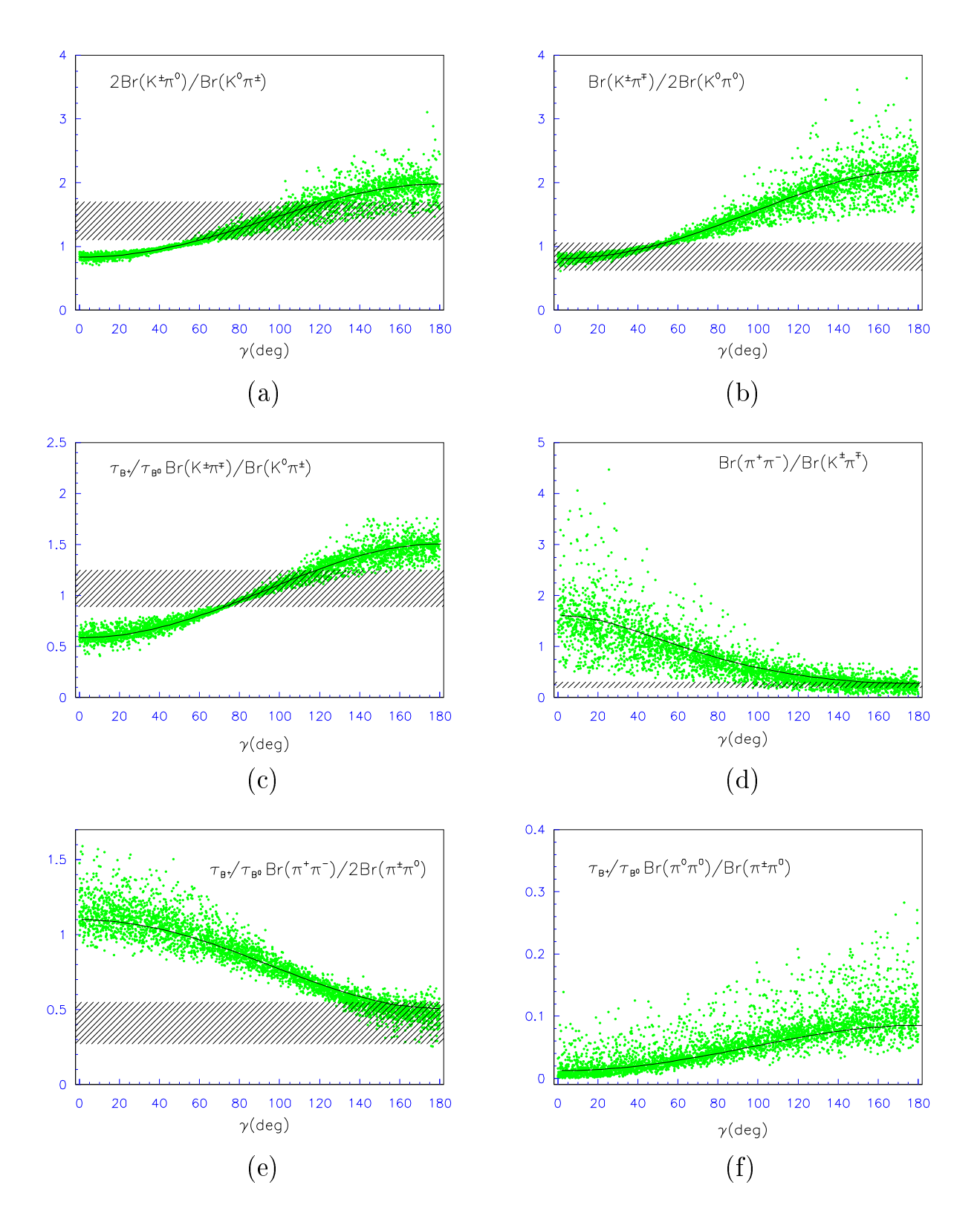


Figure 5: Ratios of CP-averaged branching fractions versus γ . The lines, bands and dot-shades have the same meaning as in Figure 3.